Biol. Cybern. 81, 425–444 (1999)

Biological Cybernetics

Recurrent V1–V2 interaction in early visual boundary processing

Heiko Neumann, Wolfgang Sepp

Universität Ulm, Abt. Neuroinformatik, D-89069 Ulm, Germany

Received: 28 October 1998 / Accepted in revised form: 19 March 1999

Abstract. A majority of cortical areas are connected via feedforward and feedback fiber projections. In feedforward pathways we mainly observe stages of feature detection and integration. The computational role of the descending pathways at different stages of processing remains mainly unknown. Based on empirical findings we suggest that the *top-down feedback* pathways subserve a context-dependent gain control mechanism. We propose a new computational model for recurrent contour processing in which normalized activities of orientation selective contrast cells are fed forward to the next processing stage. There, the arrangement of input activation is matched against local patterns of contour shape. The resulting activities are subsequently fed back to the previous stage to locally enhance those initial measurements that are consistent with the top-down generated responses. In all, we suggest a computational theory for recurrent processing in the visual cortex in which the significance of local measurements is evaluated on the basis of a broader visual context that is represented in terms of contour code patterns. The model serves as a framework to link physiological with perceptual data gathered in psychophysical experiments. It handles a variety of perceptual phenomena, such as the local grouping of fragmented shape outline, texture surround and density effects, and the interpolation of illusory contours.

1 Motivation

The brain is steadily confronted with a massive information flow that arrives via several sensory channels. In vision, pattern arrangements that signal coherent surface quantities must be somehow reliably detected and grouped into elementary items. Such a grouping enables the segregation of figural components from cluttered backgrounds as well as the adaptive focussing of processing capacities while suppressing unimportant parts of the scene (Grossberg 1980; Crick 1984).

A characteristic feature of the cortical architecture is that the majority of (visual) cortical areas are linked bidirectionally by feedforward and feedback fiber projections. So far, the precise computational role of the descending feedback pathways at different stages of processing remains largely unknown. Previous computational models incorporate feedback mechanisms to complete initially fragmented contours (Grossberg and Mingolla 1985) or, more recently, to carry top-down shape templates to generate the representation of residuals from the difference between templates and the sensory input (Mumford 1991, 1994). A comprehensive discussion of these and other approaches is given in Sect. 5.

Recent empirical evidence supports the view that top-down projections primarily serve as a modulation mechanism to control the responsiveness of cells in the primary visual cortex (Lamme 1995; Salin and Bullier 1995). Based on these findings, our model proposes computational principles of feedforward and feedback interaction between a pair of cortical areas. In the lower area, mechanisms of local feature or signal detection process the input whereas in the higher area these local measurements are integrated and matched against model information, or priors, of coarse shape outline. By way of recurrent projection, these activities feed a gain control mechanism to selectively enhance those initial estimates that are consistent with a broader visual context provided by the stimulus contour and shape outline. This facilitates the segmentation of the surface layout and figure-ground segregation. Since, so far, no all-embracing neural theory of surface perception has been developed, the proposed model contributes to a better understanding of the general computational principles involved in grouping and surface segmentation. The model links physiology and psychophysics, incorporating empirical data from both research directions, and provides a common framework for distinct perceptual phenomena.

Correspondence to: H. Neumann
(e-mail: hneumann@neuro.informatik.uni-ulm.de)

2 Summary of empirical findings

The computational model proposed here has the following key components: *feedforward* and *feedback* processing between a pair of model areas, localized receptive field processing, lateral competitive interaction, and lateral horizontal integration within areas. Empirical evidence is widespread and not entirely coherent. In order to justify the computational stages of the model, we review recent physiological and morphological findings specifically emphasizing data about cortico-cortical *feedback* processing. This summary is accompanied by recent psychophysical data on spatial grouping and interpolation that relates to broader visual contexts integrating localized measures.

2.1 Morphology and physiology

The majority of areas in the cortex are connected in a bidirectional fashion. Thus, for pairs of areas mostly a forward as well as a backward stream can be identified. The functional role of the feedback stream in the reciprocal wiring between areas is not yet clearly established. This also holds for V1–V2, the focus of our interest in this contribution. Feedforward projections from monkey V1 selectively couple cells within separate processing streams, e.g. for form, color and motion/depth (DeYoe and Van Essen 1988). The pattern of feedback connectivity shows a precise retinotopic correspondence; however, the reciprocated connections diverge from V2 to multiple clusters in V1 (Rockland and Virga 1989) and possibly enhance the integration of visual information across different channels (Krubitzer and Kaas 1989). Whether this is due to intrinsic divergent backprojection is not entirely clear. It has been concluded that indirect effects reflecting the convergence of information flow within V2 could also be the underlying reason for the substantial divergence (Rockland and Virga 1989). In the cat, Bullier et al. (1988) found that feedback connectivity to area 17 from sites in areas 18 and 19 is in precise retinotopic correspondence. Thus, the V1–V2 reciprocity may indeed be mainly guided by a point-to-point connectivity scheme as was suggested for the linking of cells in cytochrome oxidase blobs and bands (Livingstone and Hubel 1984). Concerning the processing of visual form information, it has been shown that V1–V2 forward connections link patches of similar orientation selectivity (Gilbert and Wiesel 1989). Receptive field sizes in V2 are substantially larger than those in V1 (von der Heydt et al. 1993). Horizontal connections of oriented V2 cells link targets of a wide range of orientation preference but avoid those with orthogonal orientations (Malach et al. 1994). Thus, one can conclude that the structure of the wiring scheme supports the specificity of contrast orientation and curved shape outline.

Several physiological studies (with monkey and cat) indicate that activation of the V2 feedback pathway is primarily excitatory and acts to *modulate* the output of the striate cortex (Salin and Bullier 1995). Feedback activation alone is not sufficient to drive V1 neurones if they are not stimulated by a visual feeding input (Sandell and Schiller 1982). Inactivation of area V2 reduces V1 cell responsiveness while leaving orientation and direction selectivity unimpaired (Sandell and Schiller 1982; Mignard and Malpeli 1991). It is thus believed that the modulation is excitatory such that feedback enhances activity of V1 neurones (Sandell and Schiller 1982; Salin and Bullier 1995). Recent findings in a related study by Hupé et al. (1998) strongly support this view. These authors studied the influence of feedback from area V5 to areas V1, V2 and V3 in monkey. The results demonstrate that activation of the higher area has a facilitatory effect by modulating activities in the lower areas. Feedback connections from the higher stage thus realize a *gain enhancement* or *gating* mechanism. Further evidence is gained by recent studies on figure-ground segregation. For static orientation patterns as well as motion displays, cell activities in monkey V1 are modulated in a context-dependent way (Lamme et al. 1997). The modulation is abolished when the animal is anesthetized (Zipser et al. 1997). Structure detected in higher-order areas contributes to the context-sensitive regulation of activity in a lower area such that activity modulation serves as a general mechanism for figure-ground segregation already at the early stage of V1 and V2 processing (Lamme 1995).

The modulatory influence of the visual context on the response of a target cell to an individual stimulus element has also been demonstrated. V1 cell responses to isolated optimally oriented bars are reduced if the bar is supplemented by a texture of oriented bars of the same type. Reduction is maximal for a texture defined by bars of the same orientation as in the center, weaker reduction is observed for randomly oriented bars, and even weaker effects occur for a surround pattern with orthogonally oriented bars (Knierim and VanEssen 1992). Cell responses are raised again – even beyond the level of individual stimulation – if the central element is supplied by colinearly arranged co-oriented flanking items while keeping the surround texture. The aligned bars define a perceptually salient contour segment and ''pop-out'' pre-attentively (Knierim and VanEssen 1992; Kapadia et al. 1995).

The integration or grouping of aligned items requires a mechanism of long-range interaction between oriented contrasts. Candidate mechanisms are V2 contour cells which respond to oriented contrast stimuli as well as to illusory contours of the same orientation (von der Heydt et al. 1984). The magnitude of response for illusory contours in line gratings increases monotonically with increased line density of gratings. A contour cell can be maximally excited by a physical contrast such as a bar (von der Heydt and Peterhans 1989). Such a gradual variation indicates that the strength of the feeding input mainly determines the contour cell response instead of an all-or-none classification of coherent input. V2 contour neurons have been probed with illusory-bar stimuli. They selectively respond to coherent arrangements having both half-figures of an

illusory bar intact. If one half is missing, the cell response drops to the level of spontaneous activity (Peterhans and von der Heydt 1989). This suggests that V2 contour cells signal the presence of locally coherent stimulus patterns where the response to the whole is greater than the sum of responses to individual pattern items.

2.2 Psychophysics

Perceptual organization is an elementary principle to achieve figure-ground segregation and surface segmentation. The underlying perception of various grouping phenomena has been investigated in order to understand the encoding of spatial information. Different morphologies in random dot interference patterns have been studied in Glass patterns (Glass and Pérez 1973). The detectability of local dot correlations has been suggested to be facilitated by local cortical line detectors (Hubel and Wiesel 1968), whereas the global integration might rely on neural pattern recognition mechanisms (Glass 1969). Several authors (e.g. Smits et al. 1985) suggested that dot patterns are grouped on the basis of proximity that can be measured by directionally weighted averaging, or low-pass filtering. However, the introduction of "energy" differences in feature-pair items, the inversion of contrast polarity, and the use of triple-dot items allows the disruption of a coherent perception of Glass patterns (Prazdny 1984, 1986). These effects indicate that more complex local mechanisms are involved in order to explain the results. Prazdny (1986) conjectured that local non-linear mechanisms may be supplied by top-down mechanisms. A study by Sagi and Kovaćs (1993) confirmed the contribution of a process which involves oriented long-range interactions. The detection of spatial arrangements of oriented Gabor patches within a field of distractors is facilitated by target elements which are placed and oriented along the path axis in the grouping direction (Field et al. 1993; Polat and Sagi 1994). Kapadia et al. (1995) systematically investigated contrast threshold reduction effects for target line detection. The distance along the axis of colinearity, displacement orthogonal to this axis and deviation in an orientation were critical parameters for optimal placements of flanking bars. Spatial support could be disrupted through items that destroy feature continuity.

The strength of grouping line-like items (instead of dots) also depends on stimulus features such as edge alignment, orientation, length, and contrast magnitude (Beck et al. 1989), but not on contrast polarity (Gilchrist et al. 1997). Similar selectivities have been observed as critical for the visual interpolation in illusory contour perception (Prazdny 1983; Kellman and Shipley 1991; see the overview by Lesher 1995). Surface segmentation and figure-ground segregation necessitates contour completion over gaps where fore-ground/background luminance differences are missing (Peterhans and von der Heydt 1991). Consequently, contour completion depends on discontinuities (inducers) which are oriented in the direction of the interpolated contour. Completion occurs in the same direction as the inducing contrast as well as orthogonal to line endings (Kanizsa 1976; Prazdny 1983; Shipley and Kellman 1990). Some authors claim that basic visual filtering at different spatial resolutions is the primarily mechanism for subjective contour perception (Ginsburg 1987). However, this view is challenged by investigations using stimuli (Kanizsa squares) of the same average luminance for figure and ground in which illusory figure brightening is abolished. Subjective contours remain robust, which indicates causal effects of spatial configuration as the main feature (Kellman and Loukides 1987). The strength of visual interpolation between edges depends on the ratio of physical edge (inducer) length to total contour length (Shipley and Kellman 1992). Such a mechanism is ecologically valuable since the formation of perceptual units remains invariant under changing viewing distances. This indicates that illusory contour generation is related to surface segmentation that cannot be simply explained by spatial filtering.

In all, a rich set of properties for perceptual contour and unit formation has been identified. Specific local features in stimulus configurations initiate the integration into coherent percepts. The more global mechanisms evaluate the arrangement of local responses according to relatable stimulus properties. The local effects of feature detection can already be linked to neural mechanisms such as simple and complex cell processing. Oriented horizontal intra-cortical long-range connections do also exist in V1. This machinery might help to explain several facilitatory effects that involve feature alignment and orientation. However, since V1 cells only connect to other cells over a distance of a few hypercolumns, one cannot explain completion, facilitation, and reduction effects that occur over ranges of 5° up to 8° visual angle (von der Heydt et al. 1993; Zipser et al. 1996). Moreover, the cause of variations in the strength of perceptual contours depending on various local and global stimulus features remains unknown. Neither do we have a solid theory of neural mechanisms of surface perception. Taken together, this calls for additional mechanisms that involve much larger spatial integration fields. Rather informal experiments highlight how local stimulus elements appear perceptually different depending on more global configurations and context. Barrow and Tenenbaum (1981) demonstrated how identical shading gradients represent different surface curvatures depending on changing shapes of object silhouettes. Similarly, Mumford (1994) showed how a given shading patch appears differently depending on the global surface arrangement. Perceptual elements can be absorbed by the structure of the whole such that a perceiver cannot even see it anymore (Kanizsa 1968). This again indicates that more global aspects of visual stimuli influence local feature measurements. We suggest that recurrences provide "... a plausible functional role for the ubiquitious feedback pathways in visual cortex, that of providing a broader context for the firing of cells in lower areas." (Knierim and Van Essen 1992, p. 978).

3 Computational model

3.1 Functionality and computational mechanisms

We suggest that the variety of empirical findings can be explained within a framework of basic computational mechanisms. In the ascending processing stream, the local contrast orientation is initially measured by cells with oriented receptive fields (RF), such as cortical simple and complex cells. Thus, for a pair of bidirectionally connected cortical areas (V1 and V2 in our case) the "lower" area serves as a stage of feature measurement and signal detection. Activities from local measurements are subsequently contrast enhanced and normalized by a mechanism of divisive inhibition (Fig. 1a; compare with Heeger 1992 and Heeger et al. 1996). The resulting activations are fed forward to the "higher" area where they are subsequently integrated by cells utilizing oriented long-range RF integration. Due to their increased RF size, such an integration along an oriented path bridges gaps including those corresponding to perceived illusory contours. The effectivity of local integration is based on a multitude of stimulus features, such as relative spatial position, alignment, and local orientation. An arrangement of items in a spatial neighborhood of a target cell facilitate its response in a graded fashion. A significant contrast element in a particular configuration is likely to occur in conjunction with other items that are arranged curvilinearly. Thus, on a functional level, the weighting pattern of these RFs can be viewed as to embody the laws of spatial proximity, good continuation, and similarity that have been qualified as perceptual rules by the Gestaltists (Koffka 1935). The effective weightings between the target location and other elements in a space/orientation neighborhood should encode the likelihood of occurrence of smooth stimulus shape segments. In other words, spatial weightings of V2 cells with oriented long-range selectivity represent "models" of visual entities, or local gestalts, that frequently occur in regular visual form patterns (Fig. 1b; compare with Grossberg and Mingolla (1985) and Zucker (1985) for first models of oriented space/orientation integration). The "higher" area locally matches "model templates" (or priors; see Mumford 1994) of expected visual structure against the incoming data carried by the ascending pathway.

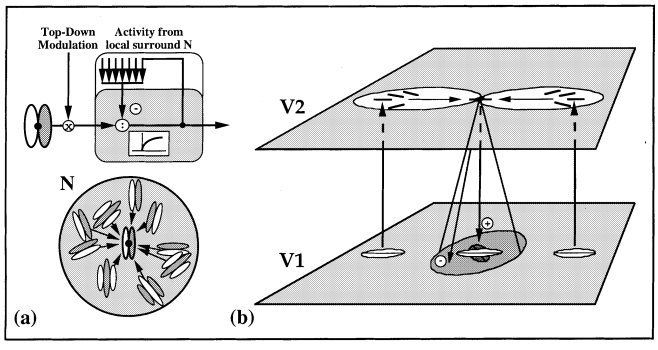

Fig. 1. Model components. (a) Feeding input is processed by localized V1 cells with oriented receptive fields whose responses are modulaed by top-down activation. Responses are subsequently normalized by a shunting competition among cells in a local neighborhood N (compare Heeger et al., 1996). (b) Model V2 cells resembling 'contour templates' integrate V1 activations from elongated RF branches. The example case shows two horizontally oriented V1 complex cells each sending their activity to one lobe of V2 cell RF. Once the V2 target cell at the center location is activated from both branches it sends excitatory feedback activity (+) to a V1 cell at the corresponding position and orientation. Inhibitory activity (−) is sent to cells in the local space/orientation neighborhood thus realizing a recurrent ON-center/OFF-surround interaction. The coaligned similarly oriented items signal the presence of a salient shape outline. In the computational scheme the activity of the central horizontally oriented cell is strengthened by the influence of flanking coaligned items. V2 cells sample the feedforward input configuration generated by V1. The individual flanking V1 cells therefore also receive excitatory input from V2 contour cells at their corresponding locations

The matching process generates an activity pattern in the higher area that is propagated backwards via the descending feedback pathway. In V1 responses of cells that match position and orientation of activated V2, contour cells are selectively enhanced; those that do not are inhibited (Fig. 1b). Thus, any feedback activation signals the degree of consistency between local measurements and model expectations (Grossberg 1980). Such expectations are generated by the spatial arrangement of localized contrast activity in a local neighborhood that is sampled by the oriented lobes of V2 cell RFs. Feedback is modulatory realizing an excitatory gain control mechanism that enhances already active cells in V1 (compare Hupé et al. 1998). The modulation is accompanied by competitive interactions to realize a "soft gating" mechanism that selectively filters activities corresponding to salient input arrangements while suppressing spurious signals that are inconsistent with the top-down priors or shape templates. The computational competence of the proposed recurrent scheme is thus to preferentially enhance those localized items that are part of a coherent arrangement of shape outline. Evidence for the presence of such an outline is accumulated by the weighted integration of measurements in an oriented space/orientation neighborhood.

3.2 Description of mechanisms

We implemented the model architecture to demonstrate the functionality of interaction between areas V1 and V2. All network levels are modeled as consisting of single compartment cells with gradual saturation-type first-order activation dynamics.

3.2.1 Model V1

At the initial measurement stage of model area V1, input luminance stimuli are processed by oriented masks of local contrast direction resembling cortical simple cells (Hubel and Wiesel 1968). We utilize linear simple cell models with odd-symmetric RF profiles for $K = 8$ different orientations, $\theta = k\pi/K$ with $k = 0, 1, \ldots, K-1$. Responses of simple cells sensitive to opposite contrast polarity, $s_{i\theta}^{\mathrm{LD}}$ and $s_{i\theta}^{\mathrm{DL}}$ [for light-dark (LD) and dark-light (DL) selectivity, respectively], are subsequently pooled to generate complex cell responses, $c_{i\theta}$, selective to

orientation but insensitive to local contrast polarity. Subscript i denotes the spatial location.

Complex cell responses are fed to a sequence of competitive interactions in model area V1, the first stage of which modulates the output of oriented contrast detection through feedback activation generated by V2 contour cells. This recurrent processing generates activities $l_{i\theta}^{(1)}$ by the following shunting interaction;

$$\frac{\partial}{\partial t} l_{i\theta}^{(1)} = -\alpha_1 l_{i\theta}^{(1)} + \beta_1 c_{i\theta}\left(1 + C\left\{h^{(2)} * \Psi^{+}\right\}_{i\theta}\right) - \zeta_1 l_{i\theta}^{(1)}\left\{h^{(2)} * \Psi^{-} * \Lambda^{-}\right\}_{i\theta} . \quad (1)$$

The constants α_1, β_1 and ζ_1 define the parameters of the dynamics of cell interaction, where α_1 determines the activity decay and β_1 and ζ_1 denote constant shunting parameters for excitatory and inhibitory response amplitudes, respectively. The constant C represents the gain factor of top-down modulation via V2 contour cell activations. Weighted averaging of activities is denoted by a convolution operation ($*$) utilizing weighting functions Λ and Ψ in the space and orientation domains, respectively. Excitatory and inhibitory interactions are denoted by '+' and '−', respectively.

Activities $h_{i\theta}^{(2)}$ denote feedback activations delivered by the descending pathway. The scheme resembles a recurrent ON-center/OFF-surround anatomy similar to the type analyzed by Grossberg (1973). In our model, the feedback mechanism, is also selective to the orientation domain (compare Fig. 1b). Closer inspection of Eq. (1) demonstrates that the enhancement via feedback activation is only effective at those positions with non-zero V1 complex cell response. Such a modulatory interaction is similar to the linking mechanism proposed by Eckhorn et al. (1990). The spatial shape and extent of inhibitory interaction follows a Gaussian distribution consistent with recent investigations by Kastner et al. (1996). In contrast to approaches such as those of Grossberg and Mingolla (1985) and Grossberg et al. (1997), in our model no activity spreading or completion occurs for locations between inducing elements of a salient perceptual contour arrangement. Thus, here the computational competence of feedforward and feedback interaction is the context-sensitive selection and enhancement of early signal and feature measurements.

The top-down modulated activities subsequently undergo a second stage of shunting ON-center/OFF-surround competition between activities in a spatial and orientational neighborhood

$$l_{i\theta}^{(2)} = \frac{\beta_2 l_{i\theta}^{(1)} - \delta_2\left\{l^{(1)} * \Psi^{-} * \Lambda^{-}\right\}_{i\theta}}{\alpha_2 + \zeta_2\left\{l^{(1)} * \Psi^{-} * \Lambda^{-}\right\}_{i\theta}} , \quad (2)$$

where α_2, β_2, δ_2, and ζ_2 are constants. With this competitive interaction, the initial top-down modulated activities are contrast enhanced and normalized by subtractive and divisive inhibition. Together, simple-cell processing, enhancement, and subsequent normalization is consistent with recent experimental and theoretical work (DeAngelis et al. 1993). Without incorporating any auxiliary compressive signal function, as suggested in other models (Heeger 1992; Heeger et al. 1996), model V1 cells generate locally normalized responses that have been selectively enhanced by a context-dependent modulating input from cells in model V2 (Knierim and Van Essen 1992). In all, the combination of both competitive processing stages in model V1 generating activities $l_{i\theta}^{(1)}$ and $l_{i\theta}^{(2)}$ realizes a *soft*-gating mechanism: V1 activities which are selectively enhanced by matching V2 contour cell activation in turn provide more inhibitory energy in the normalization stage. Thus, salient contrast arrangements will be enhanced while at the same time spurious and perceptually irrelevant responses will be suppressed by way of inhibition. In Appendix 1, we present details of this soft-gating mechanism.

3.2.2 Model V2

Arrangements of graded contrast activities are fed forward to orientation-selective contour cells in area V2. Local contrasts appear as part of smooth continuously shaped contour outlines. Therefore, a significant response measured by localized contrast cells is frequently part of a curvilinear arrangement of co-occurring contrast cell responses. The presence of coherent outlines of different curvature is encoded in a weighting pattern of connectivity that preferentially links cells of smooth contours in a space/orientation domain which tangentially pass through the target location. An oriented RF weighting function of a contour cell is thus considered as "contour template" (compare Mumford 1994) to match the likely presence of smooth shape outlines. Using this mechanism, in the first stage of model V2 the significance of a target cell response for a given orientation is evaluated on the basis of the accumulation of weighted input in the spatial neighborhood. In order to reduce the uncertainty of measurement along its axis of elongation, we partition the "contour template" into several components. Each component contributes to the final matching activity of the V2 target cell. We designed the connectivity structure of such cells taking into account that they connect with a fan-like spread and link with other cells having a wide range of orientation preferences but avoiding orthogonal orientation domains (compare Malach et al. 1994). The weighting functions define a bipartite RF by sampling opposite half-planes along their symmetry axis utilizing separate lobes (see Fig. 2a). A non-linear accumulation stage subsequently integrates the activities from a colinear pair of lobes (Grossberg and Mingolla 1985; Peterhans and von der Heydt 1989) which requires input activation from *both* branches. Functionally, such a mechanism implements an AND-gate of activities from opposite half-planes such that a contour cell only becomes activated if it signals a continuous contour segment (Fig. 2b). This is consistent with physiological findings about non-linearities in the response of V2 contrast cells (e.g. von der Heydt et al. 1984; see Sect. 2).

The weighting functions of both branches consist of ON- and OFF-subfield components (Fig. 2c) denoted by $\Gamma_{i\theta}^{\pm,L}$ and $\Gamma_{i\theta}^{\pm,R}$, respectively. ON-subfields display the pattern of *excitatory* weightings in space/orientation for "relatable"

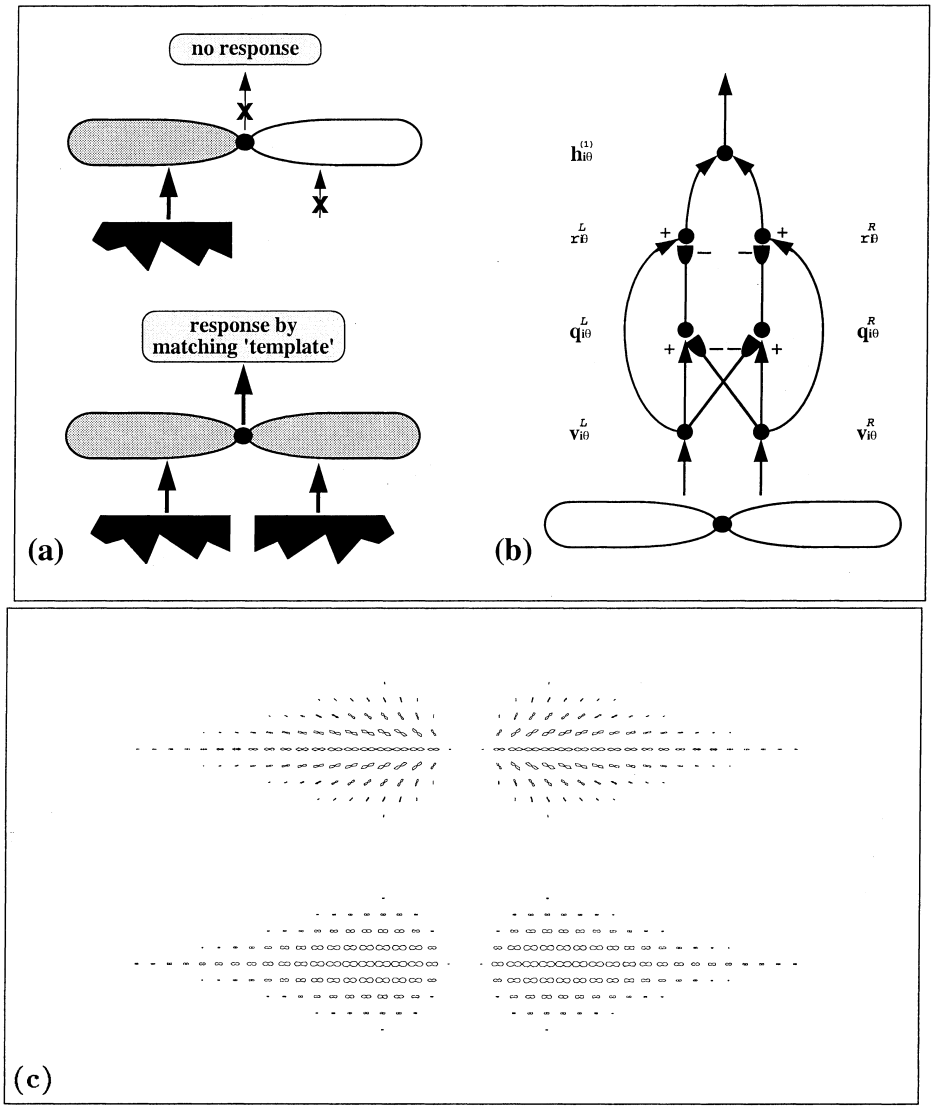

Fig. 2. Integration of input activation in position/ orientation space utilizing contour cell RFs with bipole subfield organization. (a) No target cell response is elicited if forward input is supplied only from one side of the RF sampling (top), in order to get the target cell activated requires input from both input branches (bottom) (compare with the model proposed by Grossberg and Mingolla (1985) and the findings by Peterhans and von der Heydt (1989)). (b) Model circuit that implements the functionality of a V2 contour cell tuned to horizontal orientation $\theta = 0$. Three sub-stages process the input activation gathered from both branches before being integrated at the final stage to generate $h_{i\theta}^{(1)}$ responses (see text for details). (c) Display of the ON (top) and OFF (bottom) subfield components of elongated weighting functions of V2 contour cells. Each particular spatial location contains a polar plot of the relative contributions of cells from different orientations

contrast cells to facilitate the V2 target cell (Kellman and Shipley 1991)[1]. Figure 2c shows such a cell that is tuned to horizontal orientation. This cell is tangent to an infinite number of circular arcs of different radii. Cells in the neighborhood that are also tangentially oriented to one of these arcs provide maximal support for the target cell activation (see Appendix 2). An additional *inhibitory* weighting pattern is defined by the OFF-subfield. This incorporates the "non-relatability" constraint making the space/orientation integration more selective and tuned to aligned contrast arrangements. We investigated different patterns of inhibitory weighting, including maximal suppression for orientations orthogonal to the supportive contrast orientations. A simple scheme in which inhibitory cells are similarly oriented as the target cell provided robust results for a broad range of stimulus configurations (Fig. 2c, bottom; see Appendix 2). In order not to lose selectivity to activity patterns that are aligned along the RF symmetry axis, the excitatory weighting pattern is biased to compensate for the inhibition. Input activation from both branches of a "contour template" at position i for orientation θ is computed by the convolutions $l^{(2)} * \Gamma_{i\theta}^{\pm,L}$ and $l^{(2)} * \Gamma_{i\theta}^{\pm,R}$. Since contributions of excitatory and inhibitory weightings enter in an additive fashion, we get $v_{i\theta}^{L} = \max[\{l^{(2)} * (\Gamma^{+,L} - \Gamma^{-,L})\}_{i\theta}, 0]$ and $v_{i\theta}^{R} = \max[\{l^{(2)} * (\Gamma^{+,R} - \Gamma^{-,R})\}_{i\theta}, 0]$. Incorporating a rectification operation prevents incompatible contrast configurations from generating dominant-negative responses via OFF-subfield integration.

Our V2 RF model is based on the bipole concept of long-range interaction first suggested by Grossberg and Mingolla (1985). However, unlike their approach, we utilize a micro-circuit that realizes the functionality of an AND-gate via a mechanism of self-inhibition and disinhibition. In addition to the computation of $v_{i\theta}^{L}$ and $v_{i\theta}^{R}$

[1] Kellman and Shipley (1991) defined feature *relatability* as a property that characterizes the mutual support of individual items getting integrated to form a more abstract entity [compare with the *compatibility* constraint defined by Zucker (1985)]. Any two orientations at given spatial positions are *spatially* relatable if they can be smoothly interpolated by a curve that does not bend by more than 90° and which contains no inflection point. Any two features that do not fulfill the relatability constraint are thus labeled as *non-relatable*.

activities, two additional network stages establish the AND-gate functionality generating $h_{i\theta}^{(1)}$ responses (Fig. 2b). Consider the case in which only one branch, say the left one, receives activation. Along the left branch, initial $v_{i\theta}^{L}$ activity excites the $r_{i\theta}^{L}$ cell which is inhibited by $q_{i\theta}^{L}$. Since the opposite branch has zero-level activation, self-inhibition of $v_{i\theta}^{L}$ activity leaves the target cell unexcited. Now consider the case where *both* branches receive non-zero activation. As in the first case, initial activation from left *and* right branches generates excitations $r_{i\theta}^{L}$ and $r_{i\theta}^{R}$ that are self-inhibited via $q_{i\theta}^{L}$ and $q_{i\theta}^{R}$ activation, respectively. In addition, now cross-inhibition of self-inhibitory nodes generate a disinhibition of activity for each branch. Only now can the node at the final stage be activated to generate a $h_{i\theta}^{(1)}$ response. Over all, the mechanisms of self-inhibition of individual lobes and disinhibition of activation among subfield branches guarantee that the target cell generates a response *only* when both branches are activated simultaneously.

The different stages of the micro-circuit generate activities on the basis of steady-state shunting interactions. The net effect of a lumped representation of $h_{i\theta}^{(1)}$ cell response results in a multiplicative, or gating-like, combination of activity from both branches, $v_{i\theta}^{L}$ and $v_{i\theta}^{R}$. Formally, we get the equilibrium activity

$$h_{i\theta}^{(1)} = v_{i\theta}^{L} v_{i\theta}^{R} \frac{\frac{2}{\zeta_3} + v_{i\theta}^{L} + v_{i\theta}^{R}}{\frac{1}{\zeta_3{}^2} + \frac{1}{\zeta_3}\left(v_{i\theta}^{L} + v_{i\theta}^{R}\right) + v_{i\theta}^{L} v_{i\theta}^{R}} \quad . \tag{3}$$

In Appendix 3, we present the individual stages of the micro-circuit that generate the final response in Eq. (3). Parameter ζ_3 determines the shape of the compressive non-linear function that transforms the input activation and therefore determines the responsiveness to graded V1 input. Within the limit $\zeta_3 \to \infty$, the contour response is defined by the sum of input from both bipole branches. In all, contour cells are devices which selectively respond only for cocircularly aligned contrast arrangements measured at *both* sides of a target location. In addition, we investigated the activation in response to imbalanced input arrangements. For constant *average* input, $\bar{v}_{i\theta}$, the contour cell encodes any imbalance in the input through a monotonic reduction of responsiveness. The shape of the response function is defined by

$$h_{i\theta}^{(1)}(k) = 2\left(\bar{v}_{i\theta} - \frac{1+k^2}{\zeta_3(1-k^2)}\right) \quad , \tag{4}$$

where $k \in [0,1)$ denotes the deviation of input activity from a given average level. Thus, the cell is selective to the structural coherence of the input such that any imbalance of input from both branches reduces the response amplitude in a monotonic fashion. In Appendix 3 we present details of this investigation.

Similar to V1, $h_{i\theta}^{(1)}$ activities from the the previous matching stage undergo a center-surround competition between activations in a local spatial neighborhood over orientations to generate the new activation $h_{i\theta}^{(2)}$. A shunting mechanism realizes a saturation-type normalization by divisive inhibition. Again, we assume fast relaxation to equilibrium response such that we use the resulting steady-state response of the local first-order interaction

$$h_{i\theta}^{(2)} = \frac{\beta_4 h_{i\theta}^{(1)} - \delta_4 \left\{ h_{i\theta}^{(1)} * \Psi^{-} * \Lambda^{-} \right\}_{i\theta}}{\alpha_4 + \zeta_4 \left\{ h_{i\theta}^{(1)} * \Psi^{-} * \Lambda^{-} \right\}_{i\theta}} \quad , \tag{5}$$

where α_4, β_4, δ_4, and ζ_4 are constants. The $h_{i\theta}^{(2)}$ activations are subsequently fed back via the descending pathway to enhance the activities of initial measurements from V1 oriented contrast cells (see Eq. 1).

4 Computational experiments and simulation results

The network architecture has been implemented and tested on a variety of stimuli. All linear equations for local feedforward interaction have been solved at equilibrium. The non-linear Eq. (1) was solved numerically using a fourth-order Runge Kutta scheme with adaptive step size control (Press et al. 1989). We subsequently compared the final arrangement of responses with those acquired by an approximate scheme using fix-point iteration of equilibrated responses of Eq. (1). Yet there were no observable differences in results after four iterations of the recurrent network. Therefore, in order to reduce computing time, we have used the approximate scheme to generate the set of simulation results shown below. In Appendix 4 we summarize the equations and provide all parameter settings.

We conducted a series of computational experiments with the primary goal demonstrating the role of recurrent interaction. Specifically, we show the influence of a broader context represented by V2 contour cell activations to modulate more localized measurements at the earlier stage in V1. In addition, we investigated several phenomena summarized in Sect. 2 in order to demonstrate the explanatory capacity of the proposed model.

4.1 Initial test on an artificial stimulus

In order to demonstrate the action of recurrent feedforward and feedback interaction, we first show the behavior of the network for an artificially generated input configuration. Figure 3 (top, left) illustrates the spatial outline of the test stimulus. We utilized a dark rectangle on a light background where a small strip with the background intensity covers part of the rectangle and thus splits the figure into two segregated parts. In order to demonstrate the functionality of the recurrent scheme, we generated an input configuration of artificially generated model V1 complex cell responses. In this test case, cells are active for each spatial location inside the figure but inactive at all background locations. For an unbiased input, all orientations receive the same activation (Fig. 3, top, right).[2]

[2] At each spatial location we have cells that prefer K different discrete orientations. To visualize individual activations we display polar plots each centered at the individual spatial locations (in discrete pixel coordinates).

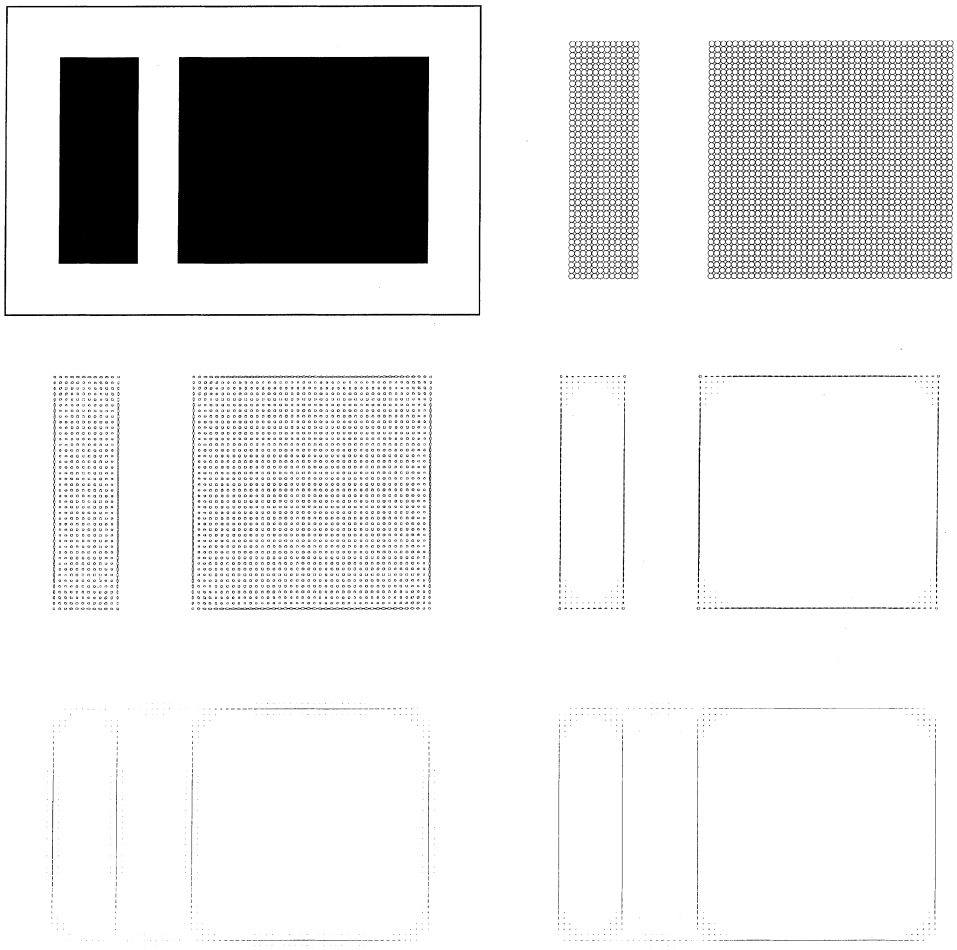

Fig. 3. Processing of an artificially generated input activity distribution. Top: Outline of test stimulus (left), synthetically generated input activity distribution (right); Center: Equilibrated model V1 cell responses, $l^{(1)}$ (left) $l^{(2)}$ (right); Bottom: Equilibrated model V2 contour cell responses utilizing elongated RFs, $h^{(1)}$ (left), and responses after normalization, $h^{(2)}$ (left). Responses saturate after four cycles of iteration

Figure 3 (center) shows the model V1 cell responses for the first stage after fusion of bottom-up and top-down pathways (left) and for the second stage after space/orientation competition and normalization (right). After four iterations, responses along the border of the compact input arrangement are enhanced and show an increased selectivity along the local boundary orientation. Responses at locations inside the region remained largely unspecific to orientation but are reduced in magnitude. After the second stage of competition, only responses along the figural boundary remained. They show a high orientation selectivity along the contours but slightly reduced activation around corners. At the vertex positions responses are increased but more unspecific with respect to orientation. This result might be attributed to a localized end-stop behavior. It should be emphasized that no additional V1 activity is generated by the recurrent interaction. Thus, feedback from a V2 cell is not an activator but rather a gain enhancer, as suggested by Hupé et al. (1998).

In Fig. 3 (bottom), model V2 cell responses are shown for the stage of the contour cells integrating feedforward V1 cell responses (left) and for the activity distribution after space/orientation competition and normalization (right). Sharp responses are generated along the outline boundary of the rectangular items. In addition, since the two segregated parts are spatially aligned, the contour integration bridges the gap to form a rectangular unit. After normalization, the weaker responses are enhanced. These boundary activations are fed back to selectively enhance those V1 activations that are consistent in position and orientation. This provides the means by which the recurrent interaction sharpens the responses generated in the lower area (model V1 in our case). Since V2 contour cells require input from both RF branches, they will be inactive at locations around corners and sharp bends. Therefore, model V2 cells do not generate any gain enhancement in the neighborhood of corners and vertices. We suggest that mechanisms selective to second-order input configurations will also contribute to the top-down process of soft gain control. This is, however, beyond the scope of the proposal reported in this paper.

In all, these simulations show the competence of each processing stage in the proposed network model. Based on these results we have further investigated the processing of real input stimuli that have been preprocessed by a stage of orientation selective contrast cells.

4.2 Texture patterns and saliency

In order to investigate the magnitude of facilitation provided by the top-down gain control mechanism we

utilized texture stimuli of the type used by Kapadia et al. (1995). We claim that the feedback of contour code patterns generates 'extra-RF modulation' of V1 responses (Zipser et al. 1996) that contributes to the surround inhibition in textures (Knierim and VanEssen 1992; Kapadia et al. 1995). An individual bar has been processed to obtain initial responses that are used as a reference. The same bar was then embedded in a texture of randomly orientated bars. Subsequently, the central bar was supplied by a row of aligned same-orientation bars (Fig. 4, left and center). Stimulus processing in model V1 generates a representation of sharply localized contrast responses for individual bar items. Model V2 contour cells generate local candidate groupings of low activation for random orientations. As a result, only minor feedback is generated for the central bar. In the stimulus with aligned bars which are supplied colinearly salient grouping is generated and a higher-order unit is formed by V2 contour processing. The resulting feedback activity selectively enhances the bar at the center of the texture. Figure 4 (right) confirms the prediction by showing the percentage change in activation in comparison to the isolated bar. In order to demonstrate the influence of the feedback gain constant C in Eq. (1), we show results for two different magnitudes. The values have been chosen to lie within the bounds derived in Appendix 1. Interestingly, an increase in the gain not only increases the facilitation in the supplement case but also increases the suppression effect for the random texture. In the model, the latter is a consequence of the stronger surround inhibition that develops in the course of several iterations at the stages of normalizing V1 and V2 cell responses, respectively.

4.3 Shape processing and contour integration

Consider a stimulus of noisy fragmented shape outline (Fig. 5, top, left; see Williams and Thornber 1997). V1 simple cells respond to luminance contrasts of individual bars. Cell responses that signal opposite contrast polarities are subsequently pooled to generate complex cell responses (Fig. 5, top, right). The subsequent stage of contrast enhancement and normalization slightly reduces the space/orientation uncertainty but still leaves a fuzzy representation of bar items. These activities are fed forward to V2 cells which match "contour templates" against the arrangement of initial responses. Those items which are part of coherent curvilinear shape outlines generate high contour activation whereas more isolated items produce only minor activation. By way of long-range integration using bipolar weighting functions, the fragmented shape is interpolated to generate a continuous representation of shape in V2. In addition, other configurations also generate candidate groupings, although represented by weaker responses compared to the central figure (Fig. 5, bottom, right). We suggest that the contrast enhanced and normalized V2 activity distribution represents an adaptive code pattern (Grossberg 1980; Mumford 1994) that is used to modulate the inital contrast measurements at V1. In other words, the activities of an interpolated shape selectively enhance initial V1 activations via an increased gain from retinotopic feedback connections. The result of recurrent feedforward/feedback processing is a distribution of sharply localized V1 contrast responses (Fig. 5, bottom, left) which, in turn, also help sharpen the interpolated contour groupings in V2.

In order to demonstrate the usefulness to deal with real world images, we show the processing results for a grey level image that has been generated in a cytological smear inspection. Figure 6 (top, left) shows the raw grey-level image taken as input. Initial contrast responses of model V1 complex cells are shown in Fig. 6 (top, right). The results of subsequent processing stages in model V1 after contrast enhancement and normalization as well as candidate groupings generated by normalized V2 cell responses are shown in Fig. 6 (bottom, left and right, respectively).

The result again demonstrates that the responses generated by V2 contour cells help to shape the orientation selectivity of V1 cells and reduce the spatial uncertainty of initial responses. Also, no extra activation

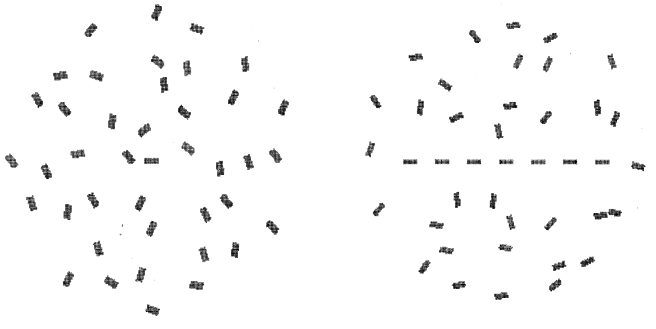

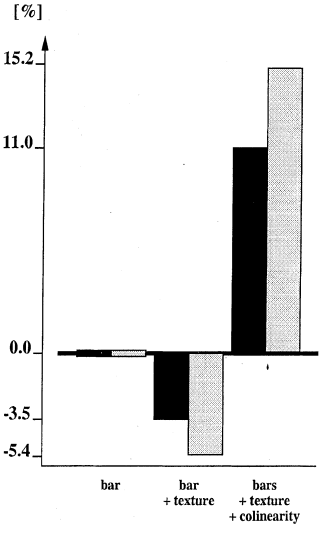

Fig. 4. Processing results for a texture stimulus composed of oriented bars. Left: Stimulus pattern with a central bar embedded in a texture with randomly oriented bar items; Center: Texture stimulus in which the central bar item is supported by aligned bars of the same orientation; Right: Equilibrated model V1 cell responses $I^{(1)}$ for the central bar as a function of the top-down gain control parameter C (see Eqn. 1) for different stimuli. Percent change in activation is shown relative to the activity in response to an isolated bar. Shaded bars display results for different values of the gain control factor C (black: C = 5, grey: C = 10)

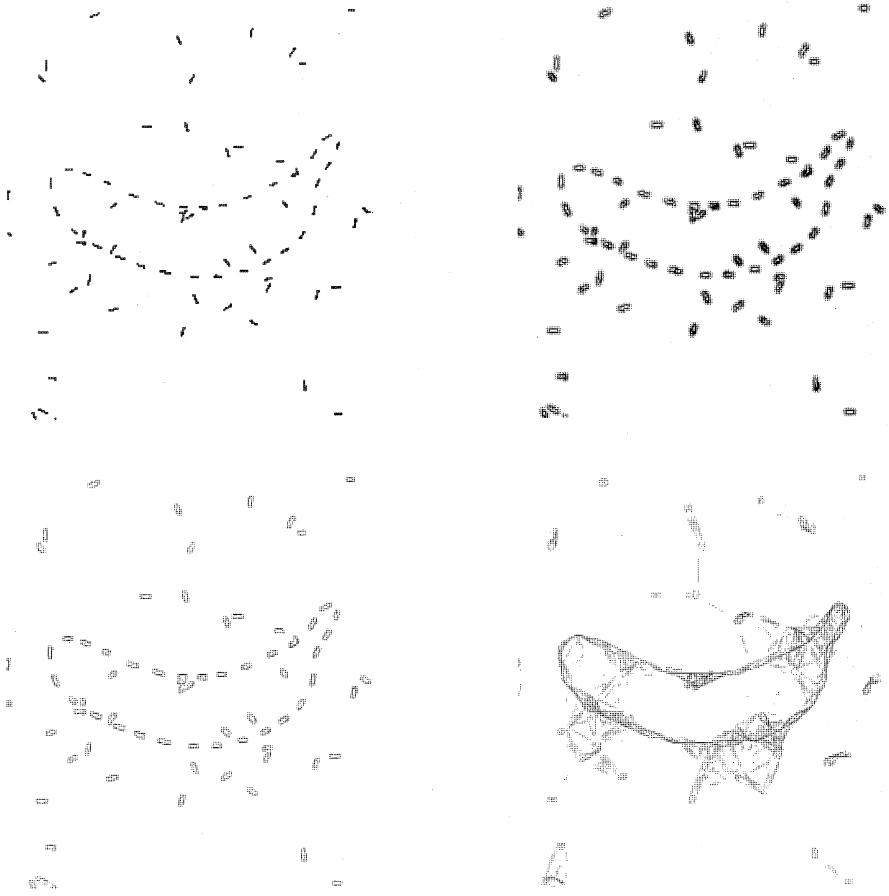

Fig. 5. Processing of a noisy fragmented shape outline (from Williams and Thornber, 1997). Top left: Input image; Top right; Responses of contrast detection stage utilizing oriented filters (complex cells), c; Bottom left: Equilibrated normalized model V1 cell responses, $l^{(2)}$; Bottom rightL Equilibrated model V2 cell responses utilizing 'contour utiling templates', $h^{(2)}$. Responses saturate after four cycles of iteration

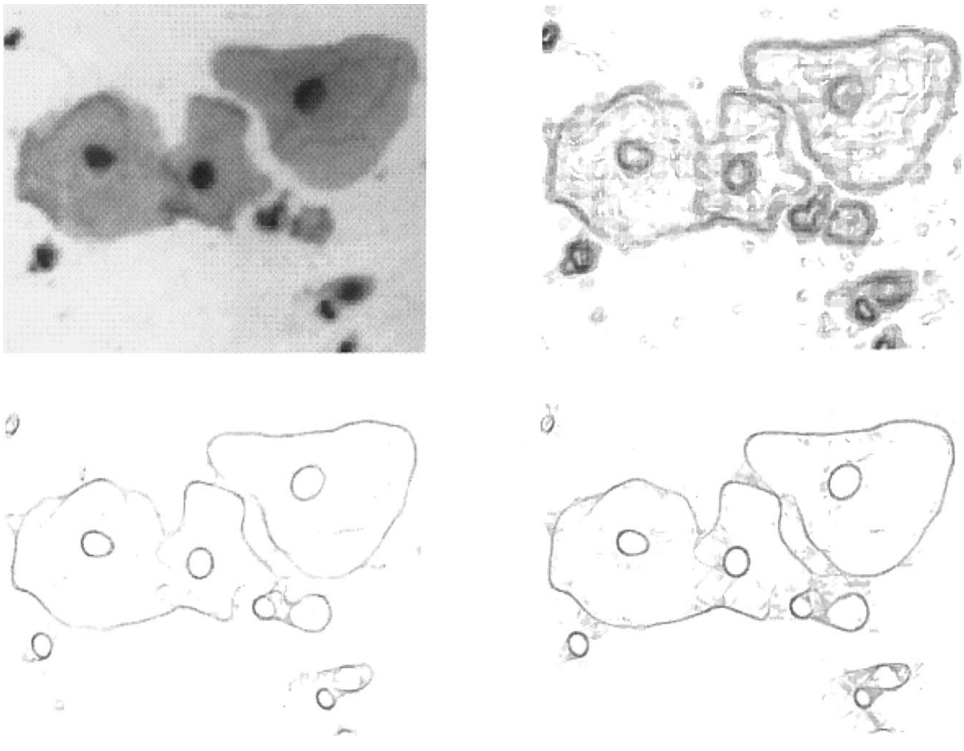

Fig. 6. Processing of a noisy grey level image from medical routine cytological smear inspections. Top left: Input image; Top right: Responses of contrast detection stage utilizing oriented filters (complex cells), c; Bottom left: Equilibrated normalized model V1 cell responses, $l^{(2)}$; Bottom right: Equilibrated model V2 cell responses utilizing 'contour templated', $h^{(2)}$. Responses saturate after four cycles of iteration

has been generated at the stage of model V1. The most salient activities have been enhanced whereas the initial clutter and spurious responses have been suppressed. Cells in model V2 respond to figural outlines represented by luminance contrasts. In addition, candidate groupings of relatable contrast elements are generated. These activations in turn are fed back to stabilize those initial estimates that are consistent with the 'expectations' that are generated by the long-range integration and grouping process.

4.4 Contour interpolation and context effects

Experiments by Baumgartner and coworkers (Baumgartner et al. 1984; von der Heydt and Peterhans 1989) have demonstrated that V2 contour cells respond to occluding contours generated by oriented abutting gratings (Fig. 7, left). Our network simulations demonstrate that V1 cells signal the boundaries of individual bars whereas, at V2, contour cells also generate sharply localized interpolations between line endings, thus generating illusory contours (Fig. 7, center and right). Our focus of investigation again is the top-down modulation of V1 measurements. We investigated the response of cells tuned to different orientations at a line ending in the center of the stimulus. Initially, responses for different orientations were rather unspecific. Thus, each individual cell shows a broad orientation tuning (compare Ringach et al. 1997). Now, the significant grouping of cell responses at V2 for the horizontal orientation kicks in and, in turn, by way of feedback gain control, selectively enhances V1 cells for the corresponding orientation ($\theta = 0$ in Fig. 8, left). V1 cell responses saturate after four cycles of iteration. Along this time course, we observe that responses for the horizontal orientation are significantly increased whereas, at the same time, responses for the other orientations are reduced.

In all, the tuning curves of the target cells were shifted by the inhibition of flanking items. Using our model such an effect can be explained as a combination of increased gain for a different dominant orientation which, in turn, increases the inhibition for a target cell. Our model predicts that, compared to a physical contrast, the illusory contour strength for the grating develops more gradually over time. Initially, since the V1 cells respond rather unspecifically, the interpolated contour should also be

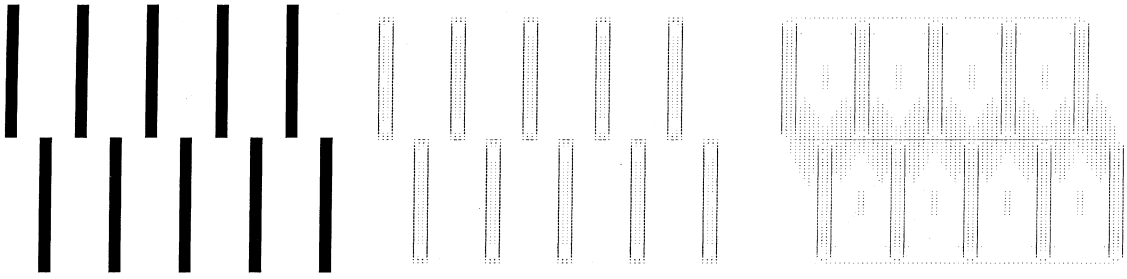

Fig. 7. Processing an abutting grating pattern composed of oriented bars. Left: Input pattern Center: Equilibrated model V1 cell responses $l^{(2)}$ that highlight the boundaires of the individual bars. Right: Equilibrated model V2 cell responses $h^{(2)}$ for the grating pattern. Cell activities are generated for horizontal illusory contour locations with high activation level at the center and with less activation at the top and bottom line (compare von der Heydt and Peterhans, 1989)

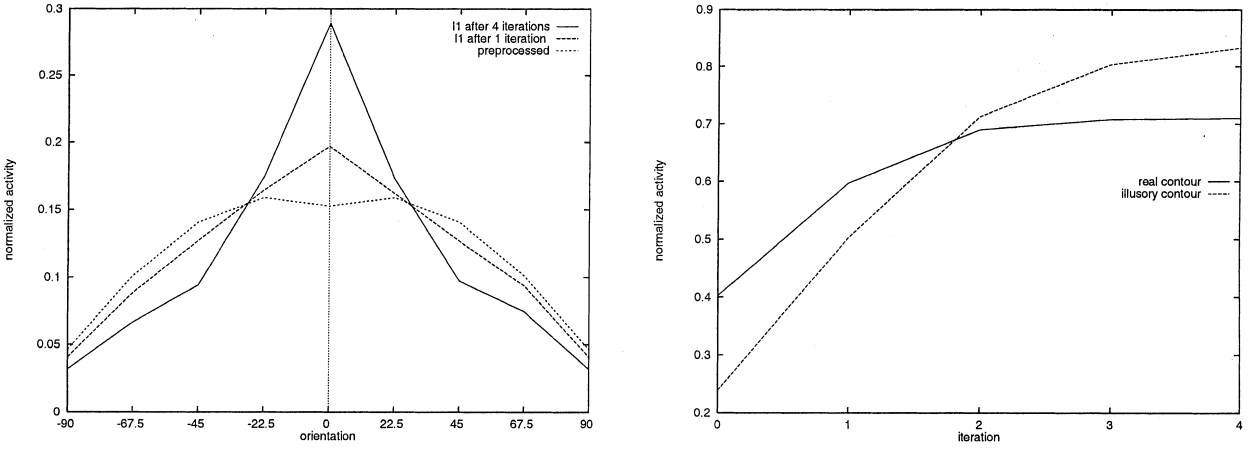

Fig. 8. Temporal evolution of cell responses. Left: Initial processing at line ends shows an unspecific $l^{(1)}$ response corresponding to a broad orientation tuning. Recurrent interactions signals a perceptually significant horizontal (illusory) contour. In the course of temporal evolution over four cycles of iteration the activity saturates with a reduced orientational uncertainty building up a dominant selectivity to these horizontal orientation. Right: Temporal development of V2 cell responses $h^{(2)}$ for a contour at real contrasts (solid curve) and an illusory contour (dotted curve)

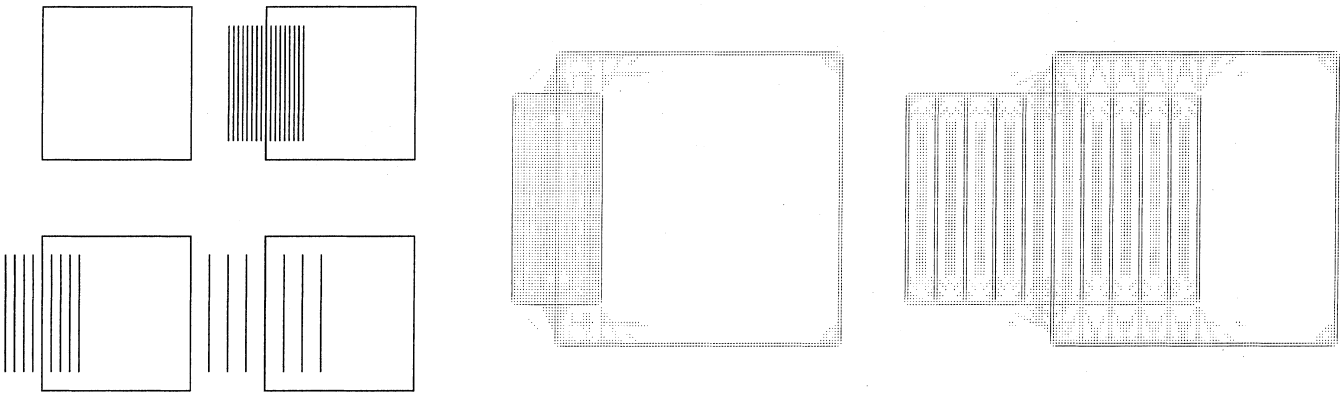

Fig. 9. Demonstration of different contour responses which depend on the local context and density of contour arrangement. Left: Input stimulus with a plain square line arrangement and three versions of the same square overlayed with texture regions of varying line densities; Center: $h^{(2)}$-responses of model V2 cells for the square line pattern with a dense bar texture which appears as a coherent surface region in front of the square; Right: $h^{(2)}$-responses of model V2 cells for the same square line pattern overlayed by a texture of wide bar separation – the region has lost its structural coherence against the square and thus the apparent occlusion and figure-ground segregation disappears

shallow. As the V1 cell selectivity is sharpened by consistent top-down enhancement, V2 contour cells generate localized responses of high amplitude. Figure 8 (right) shows this result for two selected model V2 cells. A luminance contrast is already registered in the first pass of bottom-up processing. The initial response is further enhanced to generate a saturated activity for the contour of a vertical bar. For the horizontal illusory contour in the center, the response develops more gradually. In the beginning, a minor response is present (see the discussion in von der Heydt and Peterhans 1989). This response increased over time until saturation as the responses for the horizontal orientation are progressively enhanced via feedback interaction. The saturated illusory contour response is even higher than for the luminance contrast.

A final experiment investigates the dependency of contour perception on spatial configuration effects. Figure 9 (left) shows four squares. If a borderline is surrounded by bar segments of the same thickness, the individual line of the square boundary gets lost, depending on the density of the flanking bars (compare with Kanizsa 1968). As suggested by Mumford (1994), a perceptual system should generate a representation that is in accordance with the spatial context. Thus, individual responses based on local measurements might appear different in varying contexts of visual stimulation. Figure 9 (center and right) demonstrates this for the dense arrangement as well as the wider separated flanking bars. In the first case, V2 contour cells generate a rectangular shape outline for the texture. Top and bottom endings are interpolated generating an illusory contour. The line that belongs to the square is almost absorbed by a significant reduction in contour response. If the texture bars were increasingly more separated spatially, responses were generated for individual lines. The central square line appears at the same strength as the other bars. Their perceptual belonging is represented by the interpolation between their aligned top and bottom line endings. We suggest that the mechanisms of our model therefore play an important role in surface segmentation and shape recognition.

5 Summary and discussion

5.1 Results

In this paper, we first propose a computational framework for bidirectional visual cortical processing, namely of recurrent V1 and V2 interaction, that helps to link physiology and psychophysics. Second, we present a model of modulation of initial V1 responses by context-dependent top-down V2 contour cell activation. In general, for a pair of cortical areas, the "lower area" is considered a stage of signal measurement whereas the "higher area" evaluates the significance of arrangements of local activity patterns based on context information. The results of simulations unify several seemingly unrelated experimental findings. This suggests a novel interpretation of the role of contour interpolation at V2 such that observable effects relate to the task of surface segmentation and that this information is used to evaluate and guide initial measurements at earlier stages of processing. Thus, the model links physiological and perceptual findings. Finally, we propose a unified scheme for contour integration using "contour templates" that incorporate selective subfield integration, spatial relatability constraints and cocircularity measurements.

The model predictions are consistent with a number of physiological and psychophysical findings. For example, the results for the bar texture patterns (Sect. 4.2) are consistent with the experimental findings of Knierim and VanEssen (1992) and Kapadia et al. (1995), showing a reduction of response when the bar is part of a random texture. The alignment of multiple bars outside a V1 cell RF increases the response at the target location (Kapadia et al. 1995; see also Sect. 4.3). This facilitation effect is also consistent with perceptual effects of contour detection in texture patterns (Field et al. 1993). Model simulations also predict the generation of illusory contours both along the contrast direction of inducers, such as in classical Kanizsa square patterns (simulations not shown), and of those generated orthogonal to line endings, such as for abutting gratings (Sect. 4.4). V2 con-

tour cells respond to fragmented shape outlines generated by grating bars and illusory bars (Peterhans and von der Heydt 1989, 1993). A facilitation of threshold contrast detection of the same amount has been observed for line gaps as well as illusory contours (Rieger and Gegenfurtner 1998). Moreover, the effects were independent of whole figural presentation, which suggests a contour-oriented mechanism. The processing results for grating patterns show how context effects signalled at a higher processing stage can alter the responsiveness of cells at an earlier stage. The findings are consistent with those investigating the change in orientation selectivity of V1 cells by flanking bars (Gilbert and Wiesel 1990). The responses for the grating that represent an interpolated illusory contour may be even higher than the magnitudes of those generated for physical contrasts (e.g. along the outline of an individual bar). This again is consistent with the results reported by Baumgartner et al. (1984) (see also von der Heydt et al. 1984), indicating an increased cell response to the illusory contour of abutting gratings than to a bar. We observe an increasing strength of response as a function of the number of inducing line ends. This is consistent with the data shown by von der Heydt et al. (1984). In its limit, an arrangement of one-sided line endings merges to generate a continuous luminance contrast. The simulations results in Fig. 8 (right) thus predict that the response amplitude is reduced for increased density of bars due to stronger inhibition generated by the feedback as well as the competitive interactions at the stage of V1 interaction. This, in turn, is consistent with the inverted U-shaped function of perceptual contour strength measured by Lesher and Mingolla (1993) for Varin figures with varying line density.

5.2 Related work

Our model is related to several other models. In order to achieve better readability we subdivide the discussion of other approaches according to those proposals that also incorporate a stage of oriented long-range integration (as in our model) and the discussion of more general principles and computational frameworks.

5.2.1 Recurrent processes and mechanisms of long-range integration

Other approaches have been proposed that utilize recurrent processing for contour extraction. For example, Grossberg and Mingolla (1985) proposed the Boundary Contour System (BCS), which consists of a stage of oriented contrast detection and a recurrent competitive-cooperative loop for long-range contour integration. A slightly revised version of the original BCS serves as a basic modular building block for a model of recurrent intracortical contour processing at V1 and V2 (Grossberg et al. 1997). In their model, the modular design of cortical circuits follows the suggestion that V1 and V2 circuitry are spatially homologous utilizing increased RF sizes that result in a more broadly tuned spatial scale at the higher cortical area. Oriented lateral interactions of different spatial ranges using bipole weighting functions are suggested to implement the function of horizontal connections between oriented cells in V1 and V2 layers 2/3 (Gilbert, 1992; Malach et al. 1994). Our model differs from the extended BCS in several ways. The key aspect of the development is the recurrent interaction *between* cortical areas V1 and V2. The claim is that activity integrated from separate sites in the "higher" area (model V2) is used to assess the activity distribution in the "lower" area (model V1). Thus, we suggest an instantiation of how *cortico-cortical* feedback interaction might work to evaluate initial measurements in terms of a broader visual context. Unlike the BCS, in our model contour interpolation is mainly feedforward driven without any inward spreading process that completes (or fills in) activities between inducers. Spatially segregated inducers are integrated along the bottom-up stream by space/orientation filtering using elongated bipole "contour templates". The compatibility measure that is encoded in the connectivity pattern of these weighting functions utilizes a similar support function as proposed by Parent and Zucker (1989). In order to enhance the selectivity of the support function, these authors incorporated a binary predicate to evaluate the consistency of symbolic curvature classes for candidate groupings between tangents. In our scheme, the excitatory field of cocircular tangent orientations is supplied by a field of inhibitory weightings to penalize non-relatable pairs of contrast orientation (Kellman and Shipley 1991). Furthermore, we do not include any explicit symbolic labeling of activities according to a discrete set of curvature classes. Activities that might belong to conflicting interpolations compete such that most prominent arrangements will provide strongest top-down gain. In turn, those activities compatible with such a dominant grouping will further sharpen the representation of spatially interpolated contour segments.

Similar to the BCS bipole cell functionality, but unlike Zucker's scheme, the input from the two branches is integrated in a non-linear way to resemble an AND-gate functionality. The interpolation in a feedforward process is in accordance with the model proposed by Heitger et al. (1998). However, this model and a previous version proposed by von der Heydt and Peterhans (1991) build upon selective integration of end-stop responses that are generated at corners and line terminations. This grouping stage is kept separate from processing of physical luminance contrasts. The output of the distinct activity distributions is subsequently integrated to build a final contour representation. Such a selective integration of line terminators has also been used in the model of Finkel and coworkers (Finkel and Edelman 1989; Finkel and Sajda 1992) to explicitly signal the presence of surface occlusions. Unlike Heitger's scheme, we do not utilize any segregated processing streams which selectively integrate responses from end-stop neurons. Instead, activities from initial contrast measurement are sharpened by way of feedback modulation – an option that has been abandoned in the models of Heitger and von der Heydt et al.. The result of spatial integration of contrast signals is supposed to serve as a reference, or

"expectation", to assess the significance of individual input measurements.

Zucker (1985) proposed a probabilistic relaxation scheme for iterative updating normalized contrast activities in different orientations. Each measure of locally oriented contrast is evaluated on the basis of the spatial support from contrast activations in a local neighborhood. We have instead segregated the assessment of contrast activations via a gain control mechanism and the contour interpolation into separate stages. In accordance with recent empirical data our model generates representations of visual surface contours including (illusory) contour interpolations and the context-dependent modulation of local activity measurements. Li (1998a,b) recently proposed a model of cortical contour integration. This model also utilizes oriented weighting functions for compatibility measurement in texture boundary detection. As already pointed out by Li, her model is similar to the V1 stage of processing of Grossberg et al. (1997). Li, however, demonstrated that model V1 cells – by utilizing oriented excitatory integration and local inhibition – can signal local orientation contrast and thus help to segregate regions of dissimilar texture regions. It should be noted that we do not deny the existence of oriented horizontal long-range connections at the stage of V1 processing. In fact, in the model outlined here, we wanted to focus exclusively on the issues of top-down interaction. Therefore, we excluded any additional components that might interfere with the functionality of the recurrency. Our investigation is thus complementary to these investigations as it provides the so far excluded input from extrastriate processing as suggested in our model.

5.2.2 General principles and computational frameworks

Other approaches have focussed on the integration of multiple visual cues to generate coherent percepts. For example, Edelman and coworkers have presented large scale simulations of the integration of coarse grain visual representations between segregated visual areas. Finkel and Edelman (1989) combine motion and contour processing for the generation of coherent surface percepts, whereas Tononi et al. (1992) focussed on the interaction between multiple cortical areas utilizing a lumped V1/V2 model on an even more abstract level of description. Unlike our approach, their computational strategies for dynamic conflict resolution are guided by explicit occlusion properties and associated illusory contour generation. This approach was further pursued by Finkel and Sajda (1992), who proposed linking together contrasts and surfaces in order to define object-related groupings instead of "thingless" units. We appreciate the influence of processing from even higher cortical stages, such as MT, V4 and IT, on early V1 processing of surface-related information. However, we have focussed our investigation on the more detailed mechanisms of *contour* processing among V1 and V2. Our investigation demonstrates how the dynamics of such a scheme of recurrent interaction may resolve ambiguities without the need for extra instances to handle occlusion or top-down re-entrance conflicts.

Our architecture integrates concepts of the more general computational frameworks described by Mumford (1991, 1994) and Ullman (1995). Inspired by basic principles of pattern recognition, the descending pathways in recurrent loops between cortical areas are suggested to carry flexible templates which are compared with the properties of the sensory input (Mumford 1991). A central element of this proposal is that the measure of fit between signal data and a flexible template is represented by their difference. Mumford suggested that the bottom-up pathway should carry this residual activity pattern. Rao and Ballard (1997) incorporated these concepts into a hierarchical predictor for data processing formulated in the framework of control and stochastic prediction theory. In their approach, input stimuli are processed through a hierarchical sequence of filtering stages. The output of the associated feedforward projection determines the state of the network at the subsequent model area. Given the bottom-up filtered signal data, a prediction of the expected state of the previous area is generated via a set of top-down filters. The difference between the actual activity distribution (that determines the state) and the predicted one results in a residual that is in turn filtered and fed forward again. The authors successfully demonstrated the capability of the network in object recognition tasks. They also show how end-inhibition in V1 cells might be generated by the influence of top-down feedback (Rao and Ballard 1996). It should be noted, that many of these principles are similar to the computational mechanisms in ART networks for input registration and stable category learning (Carpenter and Grossberg 1988; see Grossberg 1980 for the general computational principles). Unlike the proposal of processing residuals, mismatches are detected which subsequently trigger a reset signal to switch off activated category nodes which represent any object instances. In our model, top-down activation is rather low-level and triggered by the current stimulus configuration. Therefore, any mismatch between input activation and top-down code pattern is signalled more indirectly by a reduction in modulation strength and subsequent reduction in activity via local competitive processes. Thus, local signal measurements that do not fit the broader arrangement of contour shape are weakened or even suppressed.

The weighting pattern of our V2 contour templates is designed to support smooth contours of varying curvature. These templates are flexible in that they carry segments of frequently occurring shapes including their variance in terms of local curvature (Mumford 1994). Ullman (1995) puts emphasis on necessary testing of multiple alternatives of object hypotheses to be matched against the signal data utilizing counter-streams of bottom-up and top-down processing. We suggest that, in the case of recurrent V1–V2 interaction, the ascending pathway carries an input representation of the stimulus. The "contour templates" representing a range of curvatures are matched for different orientations. The result is a field of activities whose relative magnitudes are proportional to the degree of matching strength derived by the contour interpolation. These candidate groupings are fed back in parallel along the descending pathway to selectively

control the gain for enhancing the initial activations. Thus, we suggest that the simultaneous testing of possible alternatives (Ullman 1995; Mumford 1994) is realized by the gain-control mechanism and subsequent center-surround competition in the space/orientation domain.

5.3 Further mechanisms, limitations, and extensions

As already pointed out above, we have so far excluded any additional long-range integration at the stage of model V1. This restriction allowed us to selectively focus our investigation on the computational principles of inter-areal recurrences and the related computational competencies. We suggest that V1 long-range interaction further enhances the signal-to-noise ratio and the orientation significance of any noisy local measurement. This, in turn, would help to generate even sharper and more complete shape representations at locations with weak initial input activations. Consider Fig. 6 again. Such a mechanism might help to better signal the irregularly shaped boundary between the overlapping cells (left and center) and to close the boundary representation for the isolated cell (right). A preliminary investigation already successfully demonstrated the relevance of such a mechanism (Hansen and Neumann 1999).

The proposed scheme so far does not properly handle intrinsically two-dimensional structures (see Sect. 1). V2 model contour cells have elongated RFs which are segregated into two branches. These branches are colinearly aligned along its major axis of elongation. Input from both branches is required in order to activate a target cell. As a consequence, the cell becomes unresponsive near a corner or junction configuration where no continuous continuation in shape outline exists. We suggest that feedback from even higher stages of processing, say from area V4 or the IT cortex, can connect cells with a higher-order shape selectivity (Tanaka 1993) to those located in V1 and V2. This proposal, although speculative at the moment, appears not entirely unrealistic in principle. For example, Luck et al. (1997) have demonstrated effects of selective attention modulation of cells in V1 and V2 and Hupé et al. (1998) have shown that MT cells gate cells in previous areas such as V1 and V2. Thus, even more object-related representations with different levels of feature complexity may selectively control the responsiveness of cells at an earlier stage of processing and thus help to establish a reliable detection of junctions arrangements.

A final remark is devoted to any possible learning mechanism involved in establishing the specific connectivity pattern of contour cells. Only recently, Grossberg (1998) proposed a set of computational principles of how processes of recurrent perceptual grouping and top-down attention may interact. In our framework, V2 cell activations are considered to generate attention signals that, in turn, modulate V1 activities from long-range groupings. Such an attentive mechanism, driven by even higher processing stages (eg., V4 or IT), may also help to stabilize the early development of long-range connections of V2 cells. Consider a connected pair of presynaptic and postsynaptic cells where the efficacy, or weighting, of the connection can be modified by a local learning mechanism. Hebbian learning rewards the correlated activity of presynaptic and postsynaptic cells. In its simplest form, the weight adaptation rule is given by $\Delta\omega_{ij} = \eta y_i(t)x_j(t)$, where y_i and x_j denote activities of the presynaptic and postsynaptic neurons, respectively. In order to prevent any learning in cases where these cells are active but do not belong to an ensemble of relatable items, any weight adaptation for V2 cell inputs might be controlled on the basis of more global information. A modified version of the weight adaptation mechanism might read $\Delta\omega_{ij} = \eta k_i y_{i(t)} x_{j(t)}$ where k_i represents a function which provides an extra gain factor to properly change the weight dynamics. We suggest that k_i incorporates the V2 cell activation at location i, the corresponding V1 cell (for the corresponding orientation) and the activity of a higher stage of integrative processing (e.g., from IT). This sample case is shown mainly for illustration purposes and might be formalized by using even more elaborated mechanisms. It demonstrates, however, that the pattern of activity generated in a greater context can be used to define a semi-local learning rule for the control of Hebbian weight adaptation. It is thus conceivable that the weighting functions that have been defined for the contour cell RFs can be generated by a process of weight adaptation and learning.

5.4 Conclusion

In sum, we suggest a computational framework of how the feedback pathways might be used to assess localized measurements in previous stages of the cortical hierarchy. We particularly focussed on the recurrent processing of contour information in cortical areas of V1 and V2. In this paper, we do not attempt to develop a model that generates biologically realistic responses. Instead, the different stages represent abstractions of functionality with the goal of describing the basic computational principles of recurrent contour processing. The general principles proposed in our model are not limited to the early stage of V1 and V2. We claim that we can extend our modeling for motion as well as shape processing utilizing recurrences between areas V1/V2 and MT and V4 and IT, respectively.

Acknowledgements. We are grateful to Alexander Grunewald, Luiy Pessoa and Thomas Wennekers and to the anonymous reviewers whose insightful comments and suggestions helped to improve the presentation of the paper and to strengthen the line of argumentation.

This research work was performed in the Collaborative Research Center on the "*Integration of symbolic and subsymbolic information processing in adaptive sensory-motor systems*" (SFB-527), which is located at the University of Ulm (Germany) and is funded by the German Science Foundation (DFG). An earlier part of this investigation was supported in part by a University grant "Neue Pools" (TG 98, no. 427 98).

Appendix 1: Properties of the gain control mechanism

We investigate the enhancement and reduction of responses via the top-down feedback scheme depending on the structure of the input

configuration. In particular, we analyze the modification of an activation at a target location for one selected orientation by way of the top-down gain control mechanism. Three idealized cases will be considered: (1) the transformation of an isolated activity for a given orientation, (2) conditions for the enhancement of a localized activity that is supported by an arrangement of colinear activation, and (3) conditions for the reduction of an activation that is embedded in a dense field of co-oriented activities in a spatial neighborhood. For all input configurations, we assume unit input activation at each discrete spatial location. Since we particularly investigate one orientation field of input activation, we can neglect any cross-orientation interactions. We therefore simplify the following derivations by taking a unit weighting for the orientation fields, $\Psi^{-}_{00} = 1$.

In the first experiment, we assume a localized input activation of unit magnitude for one orientation. This setup is defined by

$$c_{i'\tau} = \begin{cases} 1 & \text{for } \tau = \theta \wedge i' = i \\ 0 & \text{for } \tau \neq \theta \vee i' \neq i \end{cases} .$$

In this case no feedback activation $h^{(2)}_{i\theta}$ is generated. We get the steady-state response of Eq. (1)

$$l^{(1)}_{i\theta} = \frac{\beta_1}{\alpha_1} .$$

The $l^{(1)}_{i\theta}$ response is a scaled version of the input. We use this level as a reference to find conditions to achieve the desired functionality of enhancement and reduction of initial responses.

In the second case, the initial response is supplied by two colinear flanking activations located at, positions $i' = i \pm \Delta$. This input configuration initiates a response at the stage of model V2 which, in turn, generates a feedback signal. This feedback activation defines the gain for enhancement of the activity at the target location. The top-down activation also contributes an inhibitory component which, in this configuration, is scaled by the connection strength at the center of the spatial weighting function Λ_{00}. We find the steady-state response

$$l^{(1)}_{i\theta} = \frac{\beta_1\left(1 + Ch^{(2)}_{i\theta}\right)}{\alpha_1 + \zeta_1 \Lambda^{-}_{00} h^{(2)}_{i\theta}} .$$

In the colinear arrangement, the initial activation should be strengthened in comparison to the case of having only an isolated input activity. We find the condition for enhancement of initial response via top-down gating by

$$C > \frac{\zeta_1}{\alpha_1} \cdot \Lambda^{-}_{00} .$$

The third case consists of a dense field of equally oriented unit amplitude input activations. Again, we find the steady-state response

$$l^{(1)}_{i\theta} = \frac{\beta_1\left(1 + Ch^{(2)}_{i\theta}\right)}{\alpha_1 + \zeta_1 h^{(2)}_{i\theta}} .$$

The response thus differs from the second condition only by an increased inhibitory contribution from the dense field of like-oriented activities. In this case now, we want to achieve a reduction of response relative to the isolated input considered in the first case. We find the corresponding condition for reduction of initial response via top-down interaction by

$$C < \frac{\zeta_1}{\alpha_1} .$$

Appendix 2: Weighting functions of "contour templates"

The connectivity patterns of the weighting functions consist of an ON-subfield as well as an OFF-subfield for each lobe of the bipole, $\Gamma^{\pm,L}_{i\theta}$ and $\Gamma^{\pm,R}_{i\theta}$. The excitatory ON-connectivity is defined for "relatable" orientations. Kellman and Shipley (1991) defined "relatability" for tangent orientations to be interpolated by a smooth curve which (1) contains no inflection point and (2) does not bend to form an acute angle. Thus, we find a range of $\theta + \alpha \leq \phi^{+} < \theta + \frac{\pi}{2}$ to be relatable at location Q. We define maximum support for contrast responses in a cocircular arrangement (Zucker 1985; Parent and Zucker 1989). Figure 10b (top) sketches the geometric arrangement of a cocircular contrast orientation at Q that is supportive for the activation at P along θ. Maximum ON-connectivity is given for cocircular arrangements at $\phi^{+} = \theta + 2\alpha$ with $\alpha = \tan^{-1}\big((y_Q - y_P)/(x_Q - x_P)\big)$. Non-relatable orientations define the OFF-connectivity in the "contour templates". The maximum inhibitory weighting is defined for $\phi^{-} = \theta$ [Fig. 10b (bottom)]. We center Gaussian weighting functions at the orientations of maximum excitatory and inhibitory strength, respectively, and define a localized excitatory influence together with a more broad inhibitory weighting, $\sigma^{+}_{\Psi} < \sigma^{-}_{\Psi}$.

The elongated spatial weighting function of "contour templates" is assembled by two subfields. The integration of curved structure in a smaller neighborhood as well as straight oriented contrast along a longer range is supplied. Each subfield weighting function can be synthesized by the superposition of an ellipse with a circle that is shifted to either end of the ellipse [Fig. 10a (bottom)]. The resulting outline contours of the spatial weighting functions are defined to follow the shape of a Poisson distribution along the axis of elongation.

Appendix 3: V2 contour cell responses

The accumulation of normalized $l^{(2)}_{i\theta}$-activities is accomplished by a micro-circuit of feedforward interaction. This circuit is designed such that an oriented V2 contour cell only becomes activated if significant input is available from *both* branches of an elongated bipartite RF (see Fig. 2). Superscripts + and − identify the individual ON-subfield and OFF-subfield weighting functions for the segregated left and right branch of a "curvature template". The weighted integration of activities in space/orientation domain is a linear process. Thus, we superimpose the ON-weight and OFF-weight by taking their difference. The single space/orientation weighting functions for left and right branches are then convolved against the normalized activity distribution of initial contrast responses. Negative responses are rectified. We get

$$v^{L}_{i\theta} = \max\left[\left\{ l^{(2)} * \left(\Gamma^{+,L} - \Gamma^{-,L}\right)\right\}_{i\theta}, 0\right], \text{ and}$$
$$v^{R}_{i\theta} = \max\left[\left\{ l^{(2)} * \left(\Gamma^{+,R} - \Gamma^{-,R}\right)\right\}_{i\theta}, 0\right] .$$

These activations are fed forward to the internal stages of the micro-circuit (see Fig. 2b). The stages of the circuit at $q^{L}_{i\theta}$ and $q^{R}_{i\theta}$, respectively, combine the activities from both bipole lobes in a cross-inhibitory fashion. We assume that the individual cell responses equilibrate fast such that we can utilize steady-state activities. In particular, for the cross-inhibition between left and right branches we have

$$q^{L}_{i\theta} = v^{L}_{i\theta}/\left(1 + \zeta_3 v^{R}_{i\theta}\right), \quad \text{and} \quad q^{R}_{i\theta} = v^{R}_{i\theta}/\left(1 + \zeta_3 v^{L}_{i\theta}\right) ,$$

where ζ_3 defines the gain of the shunting inhibitory interaction. The next stage realizes the self-inhibition of each lobe which is disinhibited if both branches are active. We get

$$r^{L}_{i\theta} = v^{L}_{i\theta} - q^{L}_{i\theta}, \quad \text{and} \quad r^{R}_{i\theta} = v^{R}_{i\theta} - q^{R}_{i\theta} .$$

Final pooling of equilibrated responses from individual input branches results in

$$h^{(1)}_{i\theta} = r^{L}_{i\theta} + r^{R}_{i\theta} .$$

Consider the case that activity is contributed by only one branch, say the left one. Activities at the first stage can be easily calculated

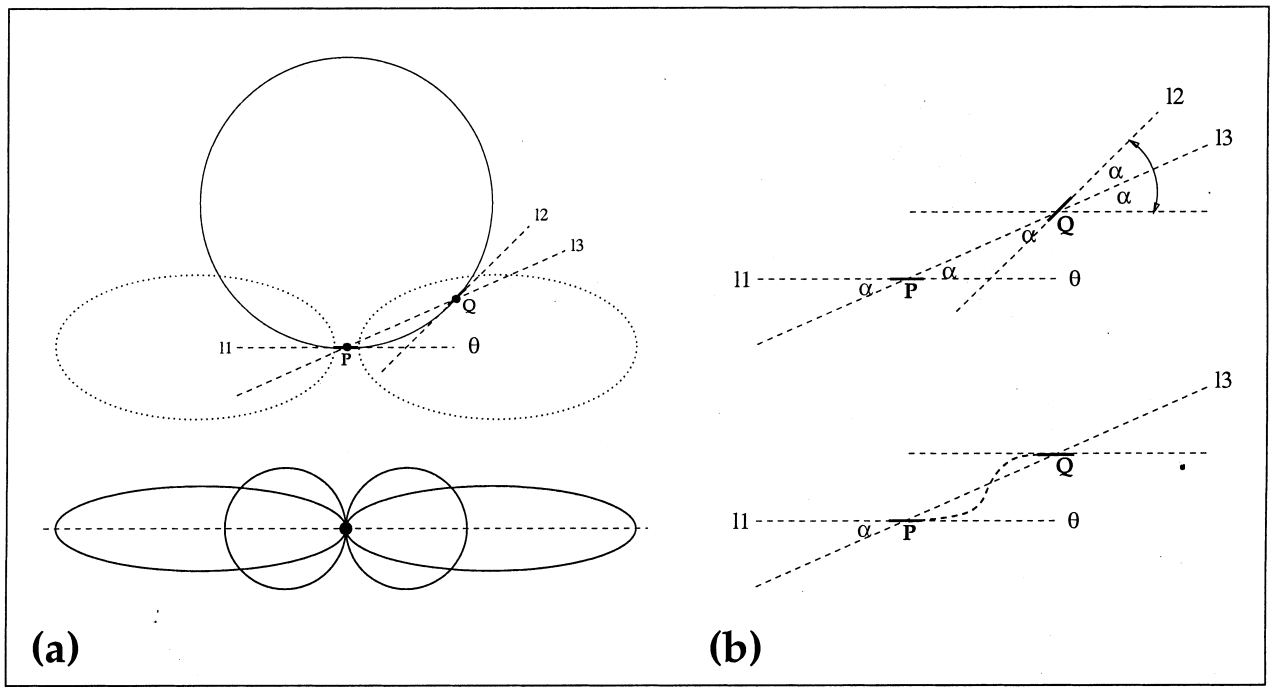

Fig. 10. Structure of bipole 'contour templates'. (a) Contour cell at position P with orientation θ; for a given location Q in the spatial neighborhood of the target cell (dashed ellipses) the orientation that is maximally 'relatable' is defined by the tangent orientation in Q of the osculating circle which passes through P and Q and is tangent to θ (top). The spatial weighting functions for the subfields are described by superimposed ellipses with shifted circular weighting (bottom). (b) Tangent orientations for a cocirular arrangement of contrast responses that define excitatory weights in the ON-subfield (top). Straight line l1 defines the orientation axis of the contour cell at P, line l3 denotes the virtual line connnecting locations P and Q, and line l2 denotes the tangent orientations that are 'relatable' and give maximum support for $\phi = \theta + 2\alpha$. The OFF-subfield defines inhibitory connections for those orientations that are not 'relatable' (bottom)

Table 1. Equations and parameter setting for initial contrast detection

Brief description $c_{i\theta}$	Model simple and complex cells for initial contrast detection (Gaussian derivative)
Responses	Simple cells (LD: light-dark, DL: dark-light):
	$s_{i\theta}^{\mathrm{LD}} = \cos(\theta)\{L*G_x\}_i + \sin(\theta)\{L*G_y\}_i$ (steering equation),
	$s_{i\theta}^{\mathrm{DL}} = -s_{i\theta}^{\mathrm{LD}}$
	Complex cells (insensitive to contrast polarity):
	$c_{i\theta} = s_{i\theta}^{\mathrm{LD}} + s_{i\theta}^{\mathrm{DL}}$
Parameter setting	Gaussian derivative kernels (5×5 pixels): $\sigma = 0.7$

Table 2. Summary of equations and parameter settings for model area V1

Brief description $l_{i\theta}^{(1)}$	Gain control via top-down activation and feedback competition
Activation dynamics	$\frac{\partial}{\partial t} l_{i\theta}^{(1)} = -\alpha_1 l_{i\theta}^{(1)} + \beta_1 c_{i\theta}\left(1 + C\{h^{(2)} * \Psi^+\}_{i\theta}\right) - \zeta_1 l_{i\theta}^{(1)}\{h^{(2)} * \Psi^- * \Lambda^-\}_{i\theta}$
Parameter settings	Shunting interaction: $\alpha_1 = 1, \quad \beta_1 = 0.42, \quad \zeta_1 = 13$
	Top-down gain factor: $C = 5$ ($C = 10$, Fig. 4)
	Weightings: Λ: $\sigma_\Lambda^- = 1.8$; Ψ: $\sigma_\Psi^+ = 0.7, \quad \sigma_\Psi^- = 2.5$
Brief description $l_{i\theta}^{(2)}$	Contrast enhancement and activity normalization via space/orientation competition
Equilibrium response	$l_{i\theta}^{(2)} = \frac{\beta_2 l_{i\theta}^{(1)} - \delta_2\{l^{(1)} * \Psi^- * \Lambda^-\}_{i\theta}}{\alpha_2 + \zeta_2\{l^{(1)} * \Psi^- * \Lambda^-\}_{i\theta}}$
Parameter settings	Shunting interaction: $\alpha_2 = 1, \quad \beta_2 = 4, \quad \delta_2 = 4, \quad \zeta_2 = 10$
	Weightings: Λ: $\sigma_\Lambda^- = 1.3$; Ψ: $\sigma_\Psi^- = 2.5$

Table 3. Summary of equations and parameter settings for model area V2

Brief description $h_{i\theta}^{(1)}$	Compatibility and weighting function for the bipole "curvature template"
Activation (final output)	$h_{i\theta}^{(1)} = v_{i\theta}^{L} v_{i\theta}^{R} \frac{\frac{2}{\zeta_3} + v_{i\theta}^{L} + v_{i\theta}^{R}}{\frac{1}{\zeta_3{}^2} + \frac{1}{\zeta_3}\left(v_{i\theta}^{L} + v_{i\theta}^{R}\right) + v_{i\theta}^{L} v_{i\theta}^{R}}$
Parameters	Shunting interaction (micro-circuit): $\zeta_3 = 15$ Spatial weightings: $\Gamma_{\Lambda}^{\text{elong}}$: $\sigma_{\text{elong}} = 8.0$, $\sigma_{\text{orth}} = 1.0$; $\Gamma_{\Lambda}^{\text{circ}}$: $\sigma_{\text{rad}} = 2.0$ Relatability: Γ_{Ψ}: $\sigma_{\Psi}^{+} = 1.0$, $\sigma_{\Psi}^{-} = 1.6$
Brief description $h_{i\theta}^{(2)}$	Contrast enhancement and activity normalization by space/orientation competition
Equilibrium response	$h_{i\theta}^{(2)} = \frac{\beta_4 h_{i\theta}^{(1)} - \delta_4 \left\{ h_{i\theta}^{(1)} * \Psi^{-} * \Lambda^{-} \right\}_{i\theta}}{\alpha_4 + \zeta_4 \left\{ h_{i\theta}^{(1)} * \Psi^{-} * \Lambda^{-} \right\}_{i\theta}}$
Parameter settings	Shunting interaction: $\alpha_4 = 1.6$, $\beta_4 = 14$, $\delta_4 = 12$, $\zeta_4 = 32$ Weightings: Λ: $\sigma_{\Lambda}^{-} = 1.6$; Ψ: $\sigma_{\Psi}^{-} = 0.5$

as $q_{i\theta}^{L} = v_{i\theta}^{L}$ and $q_{i\theta}^{R} = 0$. Self-inhibition in turn causes activities $r_{i\theta}^{L} = r_{i\theta}^{R} = 0$ such that the target contour cell remains inactivated. The micro-circuit implements the functionality of an AND-gate in which both lobes of the "contour template" must be activated in order to generate a contour cell response. If we lump together the individual stages, the final $h_{i\theta}^{(1)}$ equilibrium response of the non-linear circuit results in (see Eq. 3)

$$h_{i\theta}^{(1)} = v_{i\theta}^{L} v_{i\theta}^{R} \frac{\frac{2}{\zeta_3} + v_{i\theta}^{L} + v_{i\theta}^{R}}{\frac{1}{\zeta_3{}^2} + \frac{1}{\zeta_3}\left(v_{i\theta}^{L} + v_{i\theta}^{R}\right) + v_{i\theta}^{L} v_{i\theta}^{R}} \quad . \tag{6}$$

The activities of both lobes effectively combine in a multiplicative fashion. Parameter ζ_3 determines the shape of the non-linear transfer function to compress the input activation and therefore determines the responsiveness according to any graded V1 contrast input. Investigating the individual stages of the micro-circuit, we directly observe that a parameter setting $\zeta_3 = 0$ will eliminate the disinhibitory effect and, as a consequence, virtually inactivates the opposite lobe. As a result, contour cells will never respond. Increasing values of ζ_3 increase the disinhibitory effect of cross-channel interaction. We investigate those cases in which $\zeta_3 v_{i\theta}^{R} \gg 1$ and $\zeta_3 v_{i\theta}^{L} \gg 1$ where input configurations generate a strong cross-inhibition effect. We get $q_{i\theta}^{L} \approx v_{i\theta}^{L}/(\zeta_3 v_{i\theta}^{R})$ and $q_{i\theta}^{R} \approx v_{i\theta}^{R}/(\zeta_3 v_{i\theta}^{L})$, respectively. With *both* lobes receiving input activation we have

$$h_{i\theta}^{(1)} = v_{i\theta}^{L} + v_{i\theta}^{R} - \frac{1}{\zeta_3}\left(v_{i\theta}^{L}/v_{i\theta}^{R} + v_{i\theta}^{R}/v_{i\theta}^{L}\right) \quad . \tag{7}$$

Taking the limit $\zeta_3 \to \infty$ Eq. (7) demonstrates that the inhibitory component vanishes such that the upper limit of contour cell response is determined by the sum of inputs from both subfield branches. We define the average input $\bar{v}_{i\theta} = (v_{i\theta}^{L} + v_{i\theta}^{R})/2$. Any imbalanced input (assuming $v_{i\theta}^{L} < v_{i\theta}^{R}$) is defined relative to the constant average, such that $v_{i\theta}^{L} = (1-k)\bar{v}_{i\theta}$ and $v_{i\theta}^{R} = (1+k)\bar{v}_{i\theta}$ $(0 \le k < 1)$. The contour cell response can now be rewritten as (see Eq. 4)

$$h_{i\theta}^{(1)}(k) = 2\left(\bar{v}_{i\theta} - \frac{1+k^2}{\zeta_3(1-k^2)}\right) \quad .$$

We get equal input magnitudes from both branches for $k = 0$. For increasing values of k we see a monotonically increasing reduction of contour responses. This shows that contour cell responses are selective to the imbalance of input amplitudes from both branches. Such an imbalance can be used as a measure of structural (in)coherence in the input configuration. Equation (7) further demonstrates how contour cell responses vary for scaled contrast cell inputs. We define $v_{i\theta}^{L\,*} = m \cdot v_{i\theta}^{L}$ and $v_{i\theta}^{R\,*} = m \cdot v_{i\theta}^{R}$ and further assume $\zeta_3{}^{*} = m^{-1}\zeta_3$ (m is a scaling constant). The resulting contour cell response is scaled by the same factor m. This demonstrates that if we want to retain the functionality of the bipole integration scheme for scaled average input we have to inversely scale the gain parameter for controlling the shunting cross-inhibition.

Appendix 4

Model parameters

Tables 1, 2, and 3 display the parameter settings for the initial stage of contrast detection and the network equations of the model. The presented parameter settings have been used in all computational experiments. We split the summary into three separate parts, showing equations and settings for the initial contrast detection, model V1 and V2 cells, respectively.

References

Barrow HG, Tenenbaum JM (1981) Interpreting line drawings as three-dimensional surfaces. Artif Intell 17:75–116

Baumgartner G, von der Heydt R, Peterhans E (1984) Anomalous contours: a tool in studying the neurophysiology of vision. Exp. Brain Res (Suppl.) 9:413–419

Beck J, Rosenfeld A, Ivry R (1989) Line segregation. Spat Vis 4:75–101

Bullier J, McCourt M, Henry G (1988) Physiological studies on the feedback connection to the striate cortex from cortical areas 18 and 19 of the cat. Exp Brain Res 70:90–98

Carpenter GA, Grossberg S (1988) The ART of adaptive pattern recognition by a self-organizing neural network. Computer 21:77–88

Crick F (1984) Function of the thalamic reticular complex: the searchlight hypothesis. Natl Acad Sci USA 81:4586–4590

DeAngelis GC, Ohzawa I, Freeman RD (1993) Spatiotemporal organization of simple-cell receptive fields in the cat's striate cortex. II. Linearity of temporal and spatial summation. J Neurophysiol 69:1118–1135

DeYoe E, Van Essen D (1988) Concurrent processing streams in monkey visual cortex. Trends Neurosci 11:219–226

Eckhorn R, Reitboeck HJ, Arndt M, Dicke P (1990) Feature linking via synchronization among distributed assemblies: simulations of results from cat visual cortex. Neural Comput 2:293–307

Field DJ, Hayes A, Hess RF (1993) Contour integration by the human visual system: evidence for a local "association field". Vision Res 33:173–193

Finkel L, Edelman GM (1989) Integration of distributed cortical systems by reentry: a computer simulation of interactive functionally segregated visual areas. J Neurosci 9:3188–3208

Finkel L, Sajda P (1992) Object discrimination based on depth-from-occlusion. Neural Comput 4:901–921

Gilbert C (1992) Horizontal integration and cortical dynamics. Neuron 9:1–13
Gilbert C, Wiesel TN (1989) Columnar specificity of intrinsic horizontal and corticocortical connections in cat visual cortex. J Neurosci 9:2432–2442
Gilbert C, Wiesel TN (1990) The influence of contextual stimuli on the orientation selectivity of cells in primary visual cortex of the cat. Vision Res 30:1689–1701
Gilchrist ID, Humphreys GW, Riddoch MJ, Neumann H (1997) Luminance and edge information in grouping: a study using visual search. J Exp Psychol Hum Percept Perform 23:464–480
Ginsburg AP (1987) The relationship between spatial filtering and subjective contours. In: Petry S, Meyer GE (eds) The perception of illusory contours. Springer, New York Berlin Heidelberg pp 126–130
Glass L (1969) Moiré effect from random dots. Nature 223:578–580
Glass L, Pérez R (1973) Perception of random dot interference patterns. Nature 246:360–362
Grossberg S (1973) Contour enhancement, short term memory, and constancies in reverberating neural networks. Stud Appl Math LII:213–257
Grossberg S (1980) How does a brain build a cognitive code? Psychol Rev 87:1–51
Grossberg S (1995) The attentive brain. Am Sci 83:438–449
Grossberg S (1998) How does the cerebral cortex work? Learning, attention, and grouping by the laminar circuits of visual cortex. Boston University, Department of Cognitive and Neural Systems, TR CAS/CNS-97-023
Grossberg S, Mingolla E (1985) Neural dynamics of perceptual grouping: textures, boundaries, and emergent segmentation. Percept Psychophys 38:141–171
Grossberg S, Mingolla E, Ross WD (1997) Visual brain and visual perception: how does the cortex do perceptual grouping? Trends Neurosci 20:106–111
Hansen T, Neumann H (1999) A functional model of recurrent V1 long-range interactions. In: Bülthoff HH, Fahle M, Gegenfurtner KR, Mallot HA, (eds) Beiträge 2. Tüb. Trennmyhmungskonf. (TWK-99). Knirsch, Kirchentellinsfurt, p 62
Heeger DJ (1992) Normalization of cell responses in cat striate cortex. Vis Neurosci 9:184–197
Heeger DJ, Simonchelli EP, Movshon JA (1996) Computational models of cortical visual processing. Proc Natl Acad Sci 93:623–627
Heitger F, von der Heydt R, Peterhans E, Rosenthaler L, Kübler O (1998) Simulation of neural contour mechanisms: Representing anomalous contours. Image Vis Comp 16:407–421
Heydt R von der, Peterhans E, Baumgartner G (1984) Illusory contours and cortical neuron responses. Science 224:1260–1262
Heydt R von der, Heitger F, Peterhans E (1993) Perception of occluding contours: Neural mechanisms and a computational model. Biomed Res 14:1–6
Heydt R von der, Peterhans E (1989) Mechanisms of contour perception in monkey visual cortex. I. Lines of pattern discontinuity. J Neurosci 9:1731–1748
Hubel DH, Wiesel TN (1968) Receptive fields and functional architecture of monkey striate cortex. J Physiol (Lond) 195:215–243
Hupé JM, James AC, Payne BR, Lomber SG, Girard P, Bullier J (1998) Cortical feedback improves discrimination between figure and background by V1, V2 and V3 neurones. Nature 394:784–787
Kanizsa G (1968) Percezione attuale, esperienza passata l'"esperimento impossibile". In: Kanizsa G, Vicario G (eds) Ricerche sperimentali sulla percezione. Università degli studi, Triente, p 9–47
Kanizsa G (1976) Subjective contours. Sci Am 234:48–52
Kapadia MM, Ito M, Gilbert CD, Westheimer G (1995) Improvement in visual sensitivity by changes in local context: Parallel studies in human observers and in V1 of alert monkeys. Neuron 15:843–856
Kastner S, Nothdurfth H-C, Pigarev I (1996) The spatial extent of contextual response modulations in cat striate cortex. Soc Neurosci Abstr 22:284
Kellman PJ, Loukides MG (1987) An object perception approach to static and kinetic subjective contours. In: Petry S, Meyer GE (eds) The perception of illusory contours. Springer, New York Berlin Heidelberg, pp 151–164
Kellman PJ, Shipley TF (1991) A theory of visual interpolation in object perception. Cogn Psychol 23:141–221
Knierim JJ, Van Essen DC (1992) Neuronal responses to static texture patterns in area V1 of the alert macaque monkey. J Neurophys 67:961–980
Koffka K (1935) Principles of gestalt psychology. Routledge & Kegan Paul, London
Krubitzer LA, Kaas JH (1989) Cortical integraton of parallel pathways in the visual system of primates. Brain Res 478:161–165
Lamme VAF (1995) The neurophysiology of figure-ground segregation in primary visual cortex. J Neurosci 15:1605–1615
Lamme VAF, Zipser K, Spekreijse H (1997) Figure-ground signals in V1 depend on extrastriate feedback. Invest Ophthalmol Vis Sci 38:5969
Lesher GW (1995) Illusory contours: toward a neurally based perceptual theory. Psychon Bull Rev 2:279–321
Lesher GW, Mingolla E (1993) The role of edges and line-ends in illusory contour formation. Vision Res 33:2253–2270
Li Z (1998a) A neural model of contour integration in the primary visual cortex. Neural Comput 10:903–940
Li Z (1998b) Pre-attentive segmentation in the primary visual cortex. MIT, AI Lab, AI Memo No. 1640
Livingstone M, Hubel D (1984) Anatomy and physiology of a color systems in the primate visual cortex. J Neurosci 4:309–356
Luck SJ, Chelazzi L, Hillyard SA, Desimone R (1997) Neural mechanisms of spatial selective attention in areas V1, V2 and V4 of the macaque visual cortex. J Neurophys 77:24–42
Malach R, Tootell R, Malonek D (1994) Relationship between orientation domains, cytochrome oxidase stripes and intrinsic horizontal connections in squirrel monkey area V2. Cereb Cortex 4:151–165
Mumford D (1991) On the computational architecture of the neocortex. II. The role of cortico-cortical loop. Biol Cybern 65:241–251
Mumford D (1994) Neuronal architectures for pattern-theoretic problems. In: Koch C, and Davis JL (eds) Large-scale neuronal theories of the brain. MIT Press, Cambridge, pp 125–152
Mignard M, Malpeli JG (1991) Paths of information flow through visual cortex. Science 251:1249–1251
Parent P, Zucker S (1989) Trace inference, curvature consistency, curve detection. IEEE Trans PAMI 11:823–839
Peterhans E, von der Heydt R (1989) Mechanisms of contour perception in monkey visual cortex. II. Contours bridging gaps. J Neurosci 9:1749–1763
Peterhans E, von der Heydt R (1991) Subjective contours – bridging the gap between psychophysics and physiology. Trends Neurosci 14:112–119
Polat U, Sagi D (1994) The architecture of perceptual spatial interactions. Vision Res 34:73–78
Prazdny K (1983) Illusory contours are not caused by simultaneous contrast. Percept Psychophys 34:403–404
Prazdny K (1984) On the perception of Glass patterns. Perception 13:469–478
Prazdny K (1986) Psychophysical and computatinal studies of random-dot Moire patterns. Spat Vis 1:231–242
Press WH, Flannery BP, Teukolsky SA, Vetterling WT (1989) Numerical recipes in C/Fortran/Pascal. Cambridge University Press, New York
Rao RPN, Ballard DH (1996) The visual cortex as a hierarchical predictor. University of Rochester, Department of Computer Science, TR 96.4
Rao RPN, Ballard DH (1997) Dynamic model of visual recognition predicts neural response properties in the visual cortex. Neural Comput 9:721–763

Rieger J, Gegenfurtner K (1999) Contrast sensitivity and appearance in briefly presented illusory figures. *Spatial Vision* (in press)

Ringach DL, Hawken MJ, Shapley R (1997) Dynamics of orientation tuning in macaque primary visual cortex. Nature 387:281–284

Rockland K, Virga A (1989) Terminal arbors of individual "feedback" axons projecting from area V2 to V1 in the macaque monkey: a study using immunohistochemistry of anterogradely transported Phaseolus vulgaris-lencoagglunitin. J Comp Neurol 285:54–72

Sagi D, Kovácz I (1993) Long range processes involved in the perception of Glass patterns. Invest Ophthalmol Vis Sci 34:1130

Salin P-A, Bullier J (1995) Corticocortical connections in the visual system: structure and function. Physiol Rev 75:107–154

Sandell J, Schiller P (1982) Effect of cooling area 18 on striate cortex cells in the squirrel monkey. J Neurophysiol 48:38–48

Shipley TF, Kellman PJ (1990) The role of discontinuities in the perception of subjective figures. Percept Psychophys 48:259–270

Shipley TF, Kellman PJ (1992) Strength of visual interpolation depends on the ratio of physically specified to total edge length. Percept Psychophys 52:97–106

Smits JTS, Vos PG, van Oeffelen MP (1985) The perception of a dotted line in noise: A model of good continuation and some experimental results. Spat Vis 1:163–177

Tanaka K (1993) Neuronal mechanisms of object recognition. Science 262:685–688

Tononi G, Sporns O, Edelman GM (1992) Reentry and the problem of integrating multiple cortical areas: Simulation of dynamic integration in the visual system. Cerebr Cortex 2:310–335

Ullman S (1995) Sequence seeking and counter streams: A computational model for bidirectional information flow in the visual cortex. Cerebr Cortex: 1:1–11

Williams LR, Thornber KK (1997) A comparison of measures for detecting natural shapes in cluttered backgrounds. Proc IEEE Conf Comp Vis Patt Recog (CVPR'97)

Zipser K, Lamme VAF, Schiller PH (1996) Contextual modulation in primary visual cortex. J Neurosci 15:7376–7389

Zipser K, Lamme VAF, Spekreijse H (1997) Figure-ground signals in V1 eliminated by anaesthesia. Invest Ophthalmol Vis Science 38:S969

Zucker S (1985) Early orientation selection: tangent fields and the dimensionality of their support. Comp Vis Graph Image Process 32:74–103